Environmental Science Advances

ROYAL SOCIETY OF CHEMISTRY

CRITICAL REVIEW

View Article Online
View Journal | View Issue

Check for updates

Cite this: *Environ. Sci.: Adv.*, 2024, **3**, 1004

Advancements in the stability, protection and lead-free strategies of perovskite solar cells: a critical review

Aryan Dilawar Khan,[a] Muhammad Mustajab,[a] Sawaira Moeen,[a] Muhammad Imran,[b] Muhammad Ikram, *[a] Qasim Khan[c] and Maaz Khan *[de]

Received 28th December 2023
Accepted 21st May 2024

DOI: 10.1039/d3va00401e

rsc.li/esadvances

Lead toxicity is a challenge for the large-scale commercial production and the field implementation of photovoltaics. The fabrication of lead-free perovskite solar cells (PSCs) is environmentally acceptable; researchers have investigated the unique perovskite materials that are non-toxic in nature. The recent advancements in PSCs with suitable bandgap energy, optical and electrical features and structural alterations, methods for manufacturing metal electrodes and their internal and external effects have been investigated. Moreover, the toxic lead causes various diseases due to lead spreading in the environment which has been minimized by encapsulation. Incorporation of heterovalent and isovalent materials to reduce lead toxicity and improve stability has been discussed, and encapsulation techniques to avoid deterioration and corrosion have also been discussed. This critical review addresses the stability issues and challenges of PSCs. The intention is to pique the interest of younger researchers already active in this rapidly emerging study area.

Environmental significance

We have presented a critical review of materials with appropriate bandgap, optical, and electrical features that are either non-toxic or low-toxic and capable of maintaining their effectiveness as environmentally acceptable lead-free perovskite solar cells (PSCs). Isovalent and heterovalent metals were utilized in place of materials based on lead which will eventually lead to commercialization. Due to the poisonous nature of lead, PSCs require a suitable replacement that is also capable of maintaining its effectiveness as an alternative to lead. This review provides general knowledge of the stability issues and challenges related to PSCs. The intention is to pique the interest of younger researchers already active in this rapidly emerging area keeping in view the environmental concerns in the current days.

1. Introduction

The most important source of economic development in developed and emerging countries is energy production through renewable or non-renewable energy resources. Energy consumption has increased exponentially due to fast population growth and the high rate of per capita energy consumption.[1] Non-renewable energy resources, including oil, gas, and coal, are the primary energy sources for most of the world's population today. These energy resources pollute and harm the environment by increasing carbon emissions; as a result, it is necessary to change sustainable energy sources.[2] Solar energy is the fastest-growing sustainable energy; solar panels directly convert sunlight into electrical energy. Solar energy is cost-effective renewable energy,[3] and various technological advancements have been made to achieve energy from the sun.[4] One of the most significant obstacles to harvesting solar energy is a lack of adequate SCs with high power conversion efficiency (PCE) that can transform solar energy into usable energy.[4,5]

Perovskite solar cells (PSCs) are light-harvesting materials for photovoltaic applications and have received increased attention in 4th generation[6] solar cells (SCs). PSCs have a perfect crystalline structure, significant absorption coefficient, high bipolar mobility, long carrier diffusion lengths, modest exciton binding energy, high defect tolerance, solution processability, and low processing cost. Hybrid organic–inorganic halide perovskite materials have attracted scientific attention as next-generation light-absorbing materials with properties for energy harvesting applications.[7] PSCs have significantly reached an impressive theoretical efficiency of 30%.[8] Besides the efficiency progress and the long-term stability of PSCs, light and heat

[a]*Solar Cell Applications Research Lab, Department of Physics, Government College University, Lahore, Pakistan. E-mail: dr.muhammadikram@gcu.edu.pk*

[b]*Department of Chemistry, Government College University Faisalabad, Sahiwal Campus, Pakpattan Road, Sahiwal, 57000, Pakistan*

[c]*Department of Chemical and Petroleum Engineering, University of Calgary, Calgary, AB T2N 1N4, Canada*

[d]*Sungkyunkwan University, Suwon, Republic of Korea. E-mail: maaz@skku.edu*

[e]*Physics Division, PINSTECH, P.O. Nolire, Islamabad, Pakistan*

effects have also improved considerably in recent years, which could be attributed to the construction of a diffusion barrier against ion migration, the development of the cell encapsulation technique, and additive engineering to reduce the leakage of lead from a broken module of PSCs.[9–13] Specifically, various methods were implemented to decrease toxicity spread by the Pb, such as encapsulating procedures and substituting Pb with isovalent and heterovalent materials.[14–16] Sn-based hybrid halide perovskites appeared as a promising alternative to highly toxic Pb perovskites, demonstrating outstanding characteristics comparable to those of Pb-based perovskites, including higher adsorption coefficients and limited exciton binding energy

Aryan Dilawar Khan

Aryan Dilawar Khan, a researcher and lecturer at Shalimar Government Graduate College Lahore, Pakistan, boasts a distinguished research profile marked by his expertise in materials science. Armed with a Master of Philosophy degree from the Department of Physics and mentored by Muhamad Ikram at the Solar Cell Application Lab of GC University Lahore, Pakistan, his adeptness in leveraging fundamental materials principles at atomic and molecular scales has enabled him to engineer environmentally friendly soft nanomaterials, polymers, 2D materials, and double perovskite materials. Khan's research extends to utilizing state-of-the-art optoelectronic and dielectric applications, demonstrating his adaptability in addressing contemporary challenges in materials science. Khan's scholarly achievements serve as a testament to his impactful contributions to the scientific community.

Muhammad Ikram

Dr Muhammad Ikram obtained his PhD degree in Physics from the Department of Physics, Government College University (GCU) Lahore through the Pak-US joint project between the Department of Physics, GCU Lahore, Pakistan and the University of Delaware, USA in 2015. He served as deputy director of Manuscript Science at Punjab Textbook Board (Pakistan). Later on (in 2017), Ikram joined the Department of Physics, GC University Lahore as an Assistant Professor of Physics and Incharge of the Solar Cell Applications Research Lab. Ikram received the Seal of Excellence Marie Skłodowska Curie Actions Individual Fellowship in 2017 and 2020. Ikram recently won two national projects (NRPU, HEC, Pakistan and PSF, Islamabad, Pakistan). The PSF project Consrm-92 is entitled "Multifunctional Scaffold Materials for Highly Efficient Hybrid Halide Perovskite Solar Cells". In 2021 and 2022, Ikram was included in the 2% top scientists from Pakistan announced by Stanford University. His research interest includes the hybrid organic–inorganic solar cells, synthesis and characterization of inorganic semiconductor nanomaterials, 2D materials for water treatment, optoelectronic, and electrocatalytic applications. Ikram has published over 250 manuscripts in international well reputed journals, 15 book chapters, and published five international books.

Muhammad Mustajab

Muhammad Mustajab is working as a Research Associate at Government College University Lahore, Pakistan. He is also pursuing his PhD in Physics, with a focus on materials physics, particularly nanoscience and nanotechnology. His research endeavors focused on the synthesis of nanomaterials and their application in areas such as solar cells, water purification, water splitting, and antimicrobial activity. He is dedicated to extensively characterizing these nanomaterials, examining their morphological, structural, optical, and electrical properties to understand and optimize their performance for these applications.

Qasim Khan

Dr Qasim Khan received his PhD in Electronics Engineering from Southeast University, China, and is presently serving as Associate Research Fellow at the University of Calgary, Canada. His research focuses on 2D materials and their applications in cutting-edge optoelectronic devices such as LEDs, light-emitting FETs, and photodetectors. He has vast experience in operating various laboratory equipment for materials characterization via *sol–gel synthesis techniques, vacuum growth techniques, HR-TEM, SEM, AFM, spin-coating, UV-visible absorption spectroscopy, and electro- and photo-luminescence spectroscopies.*

sources and maximum charge-carrier mobility.[17] The SCs' efficiency and instability issues were improved to the greatest extent by improving intrinsic stability factors like the interfacial contact layer,[18] ion migration,[19] and hot carrier photogeneration.[20] The instability problem in perovskite materials was caused by moisture exposure, water, oxygen, heat, and light.[21] Moreover, despite certain benefits, a key impediment to commercialization for these types of cells is the presence of lead and its toxicity.[22] To overcome the current issues associated with lead in PSCs several techniques have been adopted, such as encapsulation and removal of Pb with suitable materials such as tin[23] and germanium[24] which belong to the same group.

This review focuses on the structure, working, and various types of layers on the PSCs. The structure of a perovskite solar cell (PSC) consists of electrodes (anode and cathode), charge transport layers, the hole transport layer (HTL), electron transport layer (ETL), and the perovskite active layer. These components are arranged in either the standard (n-i-p) or inverted (p-i-n) configurations and can have either a mesoscopic or planar structure. The stability of PSCs is influenced by internal factors, such as ion migration, interfacial contact, and hot carriers, as well as external atmospheric influences, including moisture, heat, and oxygen. Various modifications, such as encapsulation and replacing lead with isovalent and heterovalent elements, to improve the stability and efficiency of PSCs have been discussed. For each lead-free material, the crystalline structure, bandgap, photovoltaic performance, and stability of PSCs have been discussed. By comparing lead-free perovskite materials, we could predict their future development.

2. Crystal structure of PSCs

Perovskite materials have remarkable thermal, electromagnetic, and optical characteristics, and their cubic lattice-nested octahedral layered structure attracts the attention of scientists worldwide.[25] There are four potential phases of perovskite

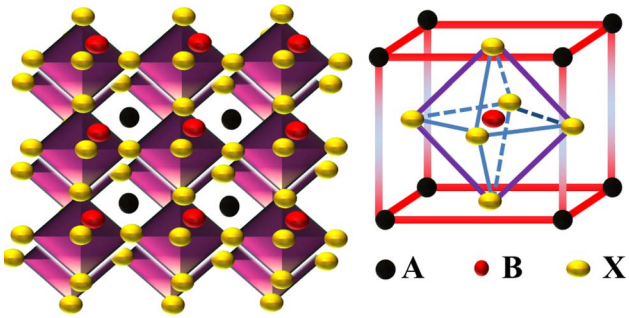

Fig. 1 Schematic diagram of the crystal structure of PSCs.[32]

configuration at various temperatures (T). The cubic phase structure is observed at $T > 327$ K, the β tetragonal phase structure is observed at temperatures less than 327 K, the γ orthorhombic phase structure appears at T equal to 160 K, and the δ polyhedral phase is a non-perovskite phase.[26] Organic and inorganic perovskite-based SCs have ABX_3 (ref. 27) crystal structures represented in Fig. 1. The crystal structure of perovskites is close to that of the mineral $CaTiO_3$ discovered in 1839.[28] The ABX_3 formula contains a large organic or inorganic cation,[27] such as methylammonium ($CH_3NH_3^+$, MA^+) or formamidinium ($CH(NH_2)_2^+$, FA^+) situated at the face-centered cubic lattices at the vertices.[26] The bonds are formed between groups A and B using inorganic cations such as copper (Cu^{2+}), tin (Sn^{2+}), and lead (Pb^{2+}), whereas X_3 refers to chlorine (Cl), bromine (Br) and iodine (I).[29,30] This led to increased interest in lead halide PSCs (LHPSCs), where the chemical composition of compound $CH_3NH_3PbX_3$ (X = Cl, Br, and I) is more cost-effective than that of traditional silicon SCs.[31]

3. Working of PSCs

SCs have been considered the essential component of a photovoltaic (PV) array.[33] SCs have been manufactured using semiconductor materials through the PV effect, transforming sunlight into electrical energy.[34] The fundamental mechanisms

Sawaira Moeen

Sawaira Moeen obtained BS (Physics) degree from Government College University Lahore (Punjab, Pakistan) in 2023. Sawaira completed BS research work at Solar Cell Applications Research Lab, Department of Physics, GCU Lahore (Punjab, Pakistan). Sawaira is enrolled M.Phil students and working as a Research Assistant in the same lab. Her research interest includes photovoltaics, synthesis of nanomaterials, and catalytic and photocatalytic degradation of organic dyes.

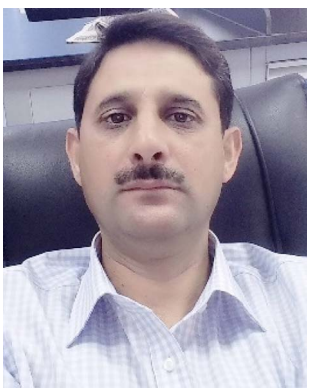

Maaz Khan

Dr Maaz Khan is working as a Professor at Sungkyunkwan University, Republic of Korea. He completed his PhD and post-doctoral research in the field of materials science (nanoscience). His research interests include the fabrication of nanomaterials and their structural, optical, magnetic, and electrical characterizations. He has authored more than 120 research articles and published 12 books. He is currently Editor-in-Chief of The Nucleus and Journal of Materials, Processing, and Design, and Executive Editor of the International Journal of Nano Studies and Technology. He serves as an editorial board member of several other materials science journals.

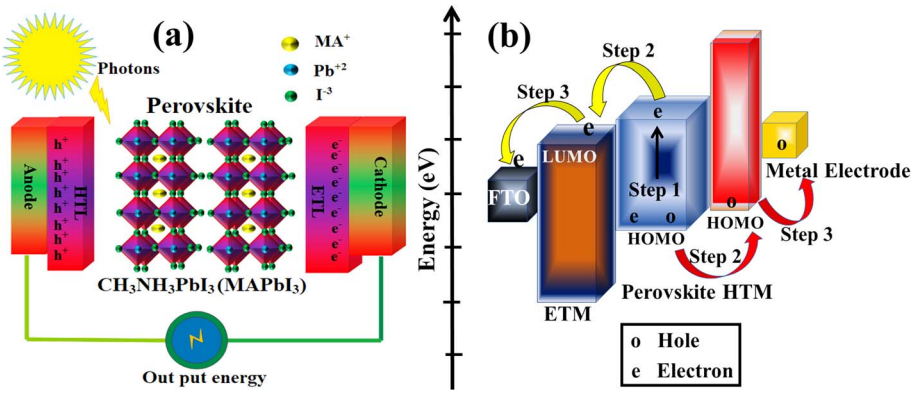

Fig. 2 (a) Working of PSCs and generation of electron–hole pairs in semiconductors, (b) energy levels in PSCs.[36]

within the SCs and the function of each layer have been discussed. Photons have more energy as compared to the band gap energy (E_g) of semiconductor materials emitted when the surface of SCs is exposed to sunlight, as can be seen in Fig. 2(a). The absorbed photons with adequate excitation energy encourage the mobility of electron–hole pairs in opposite directions in which holes move to the valence band (VB) and electrons to the conduction band (CB). Electron and hole pairs are produced in the field region and differentiated due to the field's effects. The excess electrons and holes journey through the outer circuit to reach the load. The HTL and ETL capture free holes and electrons simultaneously, accompanied by the metal electrode surface and fluorine-doped tin oxide (FTO).[35] Additionally, the electrostatic field can cause positive charges in the P-region (holes) and negative charges in the N-region (electrons), which can mitigate some of the impacts of the potential energy barrier. The free electrons in charge carriers transfer into the lowest unoccupied molecular orbital (LUMO) and then move toward the FTO or ITO, and holes in the perovskite layer transfer into the highest occupied molecular orbital (HOMO) and then move toward the metal electrode (Au, Ag) as represented in Fig. 2(b).

4. PSC material layers

The general design of the PSCs and the materials employed in their construction significantly impact the resulting device's electrical and optical characteristics. A conventional PSC device consists of five fundamental layers: perovskite active layer, HTL, ETL, transparent conductive oxide (TCO), and metal contact electrode.

4.1 Hole transport layer (HTL)

The HTL performs a crucial function in PSCs by extracting holes (positive charge carriers) from the perovskite active layer and transferring them to the top contact electrode. The HTL has been introduced between the perovskite active layer and the metal electrode layer. The HTL transfers the holes from the perovskite active layer to the metal contact electrode and blocks the entrance of electrons.[37] The HTL has a high hole mobility with an energetically desirable HOMO and LUMO for efficient charge transfer.[38] The materials used for the HTL have been divided into two categories: organic and inorganic. Organic hole transport material (HTM) based PSCs enable a high capacity for charge collection, improved crystallinity and hydrophobic nature to reduce the exposure of the perovskite layer to moisture.[39] Organic HTMs are expensive due to their difficult synthesis conditions, while hygroscopic additives cause their instability. Various polymers have been used as organic HTMs such as poly[bis(4-phenyl)(2,4,6-trimethylphenyl)amine] (PTAA)[39] and poly(3-hexylthiophene) (P3HT).[40] Inorganic HTMs provide an alternative to their organic counterparts in SC manufacturing. HTMs show potential stability compatibility with perovskite absorbers.[41] HTMs have excellent mobility of charge carriers, superior conductivity of the material in both infrared and visible regions, outstanding transmittance and high device stability, exceptional hole carrier mobility, and appropriate hole collection. Lead sulfide (PbS) quantum dots, copper oxide (CuO), copper iodide (CuI), and copper thiocyanate (CuSCN) have been employed as inorganic HTMs to enhance the stability and efficiency of SCs.[42–45]

Compared with organic polymer-based HTLs, inorganic p-type semiconductors have attained intrinsically more excellent stability. High transparency and controllable energy band alignment to the perovskite absorber layer have been observed in various materials.[46] Hybrid HTMs were manufactured by combining inorganic and organic HTMs, resulting in enhanced stability and film quality of PSCs. The use of NiO_x/PEDOT:PSS, carbon nanotube/Spiro-OMeTAD, and MoO_3/PEDOT:PSS bilayers as HTMs is proposed to enhance the effectiveness and long-term stability of heterojunction PSCs.[47–49]

4.2 Electron transport layer (ETL)

The primary function of the ETL is to make electron-selective contact with the perovskite absorber layer to increase the amount of photogenerated electron carrier. It serves as a hole-blocking layer by suppressing charge recombination as one of the most critical components for photovoltaic devices.[50] Small molecule materials hold great promise as ETL materials for fabricating low-cost and high-performance perovskite-based

optoelectronic devices under low-temperature processes.[51] The presence of an ETL provides a cascading energy level such that electrons from the perovskite absorber are transported smoothly to the cathode with little charge accumulation.[52] Electron transport materials (ETMs) should have good optical transmittance in the visible range to reduce energy loss. The energy levels of ETMs should match with the perovskite materials to improve the electron extraction efficiency and to block holes. A high-quality ETM film has good electron mobility, which is crucial for SC performance.[53]

Organic ETMs offer several benefits, including the ability to customize their optoelectronic properties by changing their structure, uncomplicated manufacturing, batch-to-batch reproducibility and flexibility. Small molecule semiconductor N-PDI can be an effective electron-transport material for achieving high-performance perovskite solar cells and drawing molecular design guidelines for electron-selective contacts with perovskites.[54] The organic materials used as ETMs are polymer, phenyl-C_{61}-butyric acid methyl ester (PCBM). When polymers are utilized as the ETL scaffold, they can offer ideal morphologies and high resistance to humidity to the perovskite absorber.[55,56] Inorganic materials typically exhibit superior thermal and long-term stability. Several durable and water-repellent inorganic materials have been employed as ETLs. The inorganic ETMs most frequently mentioned in the PSC literature are TiO_2, SnO_2, and ZnO.[57–59]

4.3 Active layer

Perovskite active layers play a significant role in the efficient performance of PSCs. The active layer absorbs photons and generates charge carriers (electron–hole pairs) that move toward the HTL and ETL, which contribute to the electrical current produced by the solar cell. Perovskites are active materials composed of organic–inorganic perovskite materials that are readily available on the planet and affordable.[60] The organic and inorganic perovskite active material can display suitable ambipolar charge transport and perform the essential tasks of PV operation, including light absorption, charge production, and movement of holes and electrons in an acceptable manner. The most often utilized perovskite active materials are $HC(NH_2)_2PbI_3$ and $CH_3NH_3PbI_3$.[61] The organic–inorganic hybrid perovskites frequently exhibit poor stability when exposed to heat, ultraviolet (UV) radiation, moisture, and oxygen. The most frequently used organic cations are MA and FA.[62] The device performance of perovskite materials is commonly impeded by their low crystallinity, resulting in a large density of defects. This, in turn, reduces the rate at which free charge carriers can diffuse, leading to charge carrier recombination, short carrier lifetime, and voltage loss.[63,64]

Therefore, in order to address the previously described limitations, other substances such as carbon-based compounds, salts, metal halides, polymers, and acids have recently been added to the perovskite film. Carbon-based materials, such as graphene and its derivatives, have the potential to be added to the perovskite active layer material. This is because they have a wide range of absorption in different light wavelengths, high ability to transport electric charges, and are stable to heat, chemicals, and mechanical stress. They have a good crystal structure and do not adversely affect the environment.[65,66]

4.4 Electrodes

The electrode materials play an important role in solar energy conversion in PSCs. The electrode materials are chemically stable and tough enough to prevent moisture from penetrating the perovskite active materials during the device fabrication. The electrode materials did not directly connect with the perovskite active materials. There are two types of electrode layers: one is a bottom contact electrode, and the other is a top contact metal electrode.

The bottom contact electrode materials contain a transparent conductive oxide (TCO) electrode with a high level of optical transmittance within the range of visible wavelengths to allow a greater amount of light to enter the cell. TCO is essential for allowing sunlight to enter the cell with little reflection or absorption and transferring the charge carriers from the active layer to the external circuit. Fluorine-doped tin oxide (FTO) and indium-doped tin oxide (ITO) are the most often utilized TCOs because of their outstanding stability, transmittance, and low sheet resistance. Additionally, they should exhibit a high level of electrical conductivity to facilitate the efficient transportation of photogenerated current to the external circuit. ITO is widely used as a transparent conductive electrode in PSCs due to its high electrical conductivity and excellent optical transmittance in the visible region. Nevertheless, the excessive expense, limited availability, and hazardous properties of indium impose restrictions on the selection of ITO.[67,68] Novel materials, including conductive polymers, graphene, CNTs, and metal nanowires, have recently emerged as potential alternatives to the traditional ITO and FTO transparent conductive electrodes. These materials offer high optical transmittance in the visible range and comparable electrical conductivity, presenting them as promising replacements. Graphene and its derivatives have garnered significant scientific attention because they are inexpensive, non-toxic, readily available, stable, mechanically flexible, and possess a large specific surface area.[69]

The primary function of the top contact material is to gather and move charge carriers from the active layer to the external circuit, and it need not be transparent. It is situated on the solar cell's side that faces away from the light source. PSCs employ gold (Au) and silver (Ag) as the most frequently used materials for the top contact electrode. A suitable work function and resistivity were considered when selecting metals as electrodes. The contact resistances in the metal electrode should be low to maximize the PSC efficiency. A metal thin film is typically used as the top contact layer of electrodes in manufacturing PSCs with high PCE. The top contact electrode possesses excellent electrical conductivity and a work function compatible with the perovskite film and charge transport layers. Additionally, it reflects a portion of the sunlight that enters the cell, thereby enhancing photon harvesting in the perovskite active layer.[70,71]

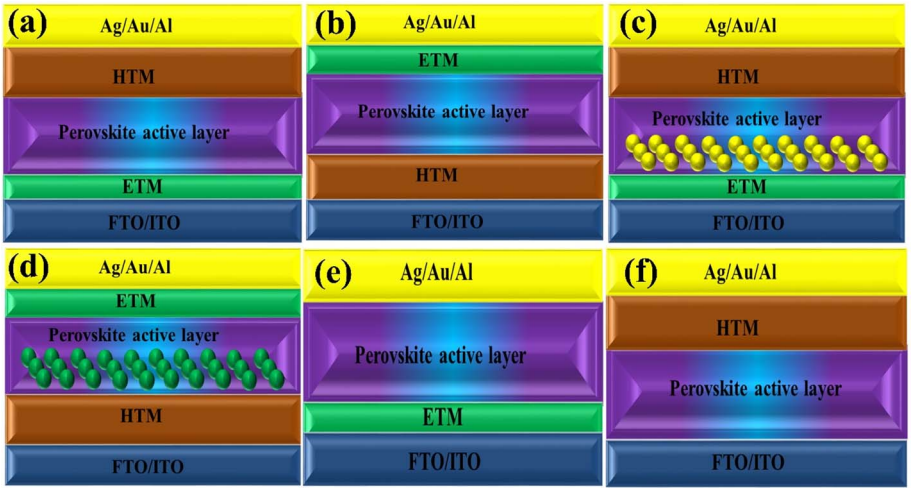

Fig. 3 The structure of PSCs are (a) planar n-i-p, (b) planar p-i-n, (c) mesoscopic n-i-p, (d) mesoscopic p-i-n, (e) HTM-free and (f) ETM-free.

5. Photovoltaic structure

PSC performance has been examined by looking at structural configuration. There are two types of PSCs: mesoscopic structures and planar structures. In the context of SCs mesoscopic structures include a mesoporous layer composed of metal oxides like TiO_2, ZnO, or Al_2O_3. Because of mesoporous layers, the structure has a vast surface area. A mesoporous layer is absent from planar structures, and there is a flat layer of material that is stacked one on top of another. The structure pair can be subdivided into normal (n-i-p) and inverted (p-i-n). Mesoscopic structures contain a mesoporous layer, whereas planar structures consist of just planar layers throughout. The use of PSCs without an ETL and HTL has also been investigated. Thus, six types of PSC structures have been studied, as depicted in Fig. 3(a)–(f): planar p-i-n, planar n-i-p, mesoscopic n-i-p, mesoscopic p-i-n, HTL-free, and ETL-free structures.

5.1 Planar PSCs (n-i-p)

Planar perovskite SCs with an n-i-p structure are a revolutionary structure in the rapidly expanding field of photovoltaics with substantial advantages in efficiency, cost-effectiveness, and scalability for solar energy harvesting applications. Planar PSCs have two perovskite interactions, perovskite/ETL and perovskite/HTL, in which electron and hole pairs effectively and speedily separate, as indicated in Fig. 3a. TiO_2 and SnO_2 are the two most extensively investigated materials used as ETMs for PSCs. TiO_2 generally suffers from low electronic mobility, and mismatched band alignment with the perovskite will induce huge hysteresis and poor ultraviolet (UV) light stability of PSCs. SnO_2 shows higher electron mobility, more suitable band alignment with perovskites, and enhanced UV light stability. By introducing RbF in an SnO_2 colloidal dispersion, the newly formed F–Sn bonds changed the electron cloud density around the Sn atoms, which helped to improve the electron mobility of SnO_2. In consequence, the PSC based on SnO_2–RbF achieved a PCE of up to 21.27%, which is mainly attributed to the increased short-circuit current density (J_{sc}).[72] SnO_2 agglomerates and produces defects and vacancies of oxygen in the film, leading to significant nonradiative recombination, diminished efficiency of the device, and noticeable hysteresis. To address these difficulties, fluoride ions have a considerable effect on passivating defects and reduce the nonradiative recombination in the perovskite absorber. SnO_2-based planar PSCs demonstrate a PCE of 20.24%, while the PSCs modified by CsF achieve a PCE of 22.51%, complemented by a practical enhancement in stability and negligible hysteresis.[73]

5.2 Planar inverted PSCs (p-i-n)

The inverted planar (p-i-n) structure is believed to account for the efficient charge carrier separation and lower charge recombination rate that produce the maximum PCE of PSCs. Numerous benefits, including simple processing procedures, excellent stability, and low hysteresis, have been achieved in planar-inverted PSCs.[74] The inverted (p-i-n) structural configurations have enormous potential and maximum performance for flexible PV devices, as shown in Fig. 3(b). To improve the performance of inverted PSCs, a variety of tactics have been employed, including crystalline management of the perovskite, generation of perovskite composition, and geomorphological control as well as modification of the charge carrier transit layers.[74]

The deposition of an ultrathin layer of PTAA and poly(3,4-ethylenedioxythiophene)–poly(styrenesulfonate) (PEDOT:PSS) has been used to achieve band energy alignment in PSCs. The ultrathin PTAA layer is significant in suppressing interfacial recombination and accelerating hole transport in PSCs; as a result, a high PCE of 19.04% with a fill factor (FF) of 82.59% and J_{sc} of 21.38 mA cm^{-2} has been achieved.[75] CuSCN-doped PEDOT:PSS acts as the HTM with a PCE of 15.3% and significantly improves stability in building inverted PSCs.[76] PEDOT:PSS can be combined with graphene quantum dots to make composites that act as a HTM in PSCs that demonstrate a PCE of 15.24% with an average value and the highest PCE of

16.15%.[77] Zheng and colleagues showed that surface-anchoring allylamine-ligands (AALs) might be used in inverted PSCs. The long-chain AAL addition to the reaction solution inhibited the non-radiative charge carrier recombination. It continued to improve the photoelectric achievement of the mixed-cation mixed-halide perovskite absorber layer, yielding an efficiently stable PCE of 22.3%.[78]

5.3 Mesoscopic PSCs (n-i-p)

The configurations of perovskite photovoltaic SCs have been investigated with the traditional n-i-p mesoscopic configuration. Mesoporous PSCs are frequently superior to their planar counterparts; typical reasons for this difference include lower hysteresis and improved charge extraction, which are commonly attributed to mesoporous conductive TiO_2. It is discovered that mesoporous insulating Al_2O_3 layers provide a tunable technique to reinforce the p- and n-character of the perovskite absorber layer by contacting the selective charge-extraction layer.[79] The structural configuration has been entirely covered with a perovskite-containing mesoporous metal oxide, accompanied by the HTM, and eventually coated with a metallic conductive anode. This initial innovation in PSCs sparked a significant interest among photovoltaic researchers, which resulted in the production of various PSC device topologies, as depicted in Fig. 3(c).

A low-cost and environmentally friendly MnS film as the HTL in mesoporous PSCs possesses high mobility of holes, tunable E_g configuration, and optical transmittance. The devices achieved a PCE of 19.86% and high-performance stability.[80] Carbon-based PSCs are rapidly progressing toward commercial manufacture. The GO used as the HTM was made using a straightforward Hummers process. Carbon acting as the back-contact electrode material in PSCs achieves an open circuit voltage (V_{oc}), J_{sc}, FF, and PCE of 0.68 V, 28.50 mA cm^{-2}, 25.8%, and 10.01% respectively.[81]

5.4 Mesoscopic inverted PSCs (p-i-n)

The mesoporous charge-transporting layers could supply heterogeneous nucleation sites for expanding high-quality perovskite crystals and an enhanced charge carrier separation region for improved charge extraction. The normal and inverted mesoscopic structures generally exhibit better performance than their planar counterparts.[82] Inverted mesoscopic PSCs have achieved significant improvements compared to the exceptionally high certified performance of mesoscopic PSCs because of the deficiency of appropriate p-type semiconductor materials for the preparation of the mesoporous HTL as can be seen in Fig. 3(d). The HTL of inverted mesoscopic PSCs can be manufactured with self-assembled nickel oxide (NiO) microspheres. These microspheres produce mesoporous NiO, which provides an efficient channel for hole extraction and transport inside the SC. The utilization of self-assembled NiO microspheres allows for the creation of efficient inverted mesoscopic PSCs with higher performance and stability. Using inverted mesoscopic PSCs in which mesoporous NiO acts as the HTL yields a PCE value of 18.17%.[82] The inverted mesoporous PSCs yield an optimal efficiency of 18.77%, which is prominent in state-of-the-art NiO-based devices that exhibit greatly improved long-term stability.[83]

5.5 Hole transport layer-free structure

HTM-free PSC architectures have a simple cell arrangement that has garnered attention in the renewable energy field. HTM-free PSCs have the potential to minimize production costs, improve stability, and increase device efficiency. Most reported high-efficiency PSCs contain costly HTMs, such as fullerenes, which significantly leads to expensive cell fabrication. Several novel HTMs were investigated with significant improvements, including small molecules, polymers, and inorganic compounds. Organo-lead halide perovskite materials have advantageous semiconductor properties such as charge transfer lifetimes and an ambipolar nature that allows the HTL to be excluded,[84] as shown in Fig. 3(e)

The HTL-free PSCs organized with chlorobenzene started shifting to a higher voltage, indicating a reduction in charge backflow at the interface. The *J–V* characteristics under illumination demonstrated that the HTL-free PSCs designed and manufactured with chlorobenzene as an antisolvent had the best PCE of 5.65%.[85] HTL-free PSCs were established in an ambient air environment. The material improved the morphology of $MAPbI_3$ films and accelerated the transfer of electrons. Combining carbon quantum dots (CQDs) and reduced graphene oxide (RGO) in a 50 : 50 ratio in the ETL caused non-radiative recombination in the $MAPbI_3$ layer, an increase in grain size, reduction in the number of grain boundaries and improvement in the photovoltaic stability and efficiency of HTL-free PSCs. Carbon nanostructures (CNSs) have demonstrated the potential to be the best candidate for enhancing the efficiency of PSCs. The combination of CNSs, RGO, and CQDs improves the productivity and stability of HTL-free PSCs in the mesoporous TiO_2 (m-TiO_2) precursor solution. Incorporating these materials in the ETL enhances the electron transfer rate and improves the surface properties of perovskite materials. The PCE and stability of the PSC were improved (from 5.88 to 10.92%) with additives.[86]

5.6 Electron-transport layer-free structure

ETL-free PSCs present a promising way to simplify device fabrication while potentially improving performance and stability. ETL-free PSCs demonstrate promising advancements in solar devices due to their elimination of the challenging and energy-/time-consuming manufacturing route of ETLs. However, ETL-free devices still perform poorly compared to traditional devices due to mismatched energy levels and unwanted interfacial charge recombination.[87]

ETL-free PSCs have low cost and large surface areas that exhibit excellent performance and stability, as shown in Fig. 3(f). ETL-free PSCs remain unsatisfactory due to several energy losses caused by mismatched ITO energy level alignment interfaces.[88] The highest PCE of 19.37% has been achieved by inserting a 5-amino-valeric acid dipole layer into the ITO/perovskite interface to transfer charge carriers at the front

interface in ETL-free PSCs.[89] ETL-free PSCs have been developed by modifying the ITO/perovskite interface with a non-toxic hypophosphorous acid dipole layer, yielding a maximum PCE of 19.32%.[90]

6. Effects of stability in PSCs

The instability of perovskite materials is a widely recognized problem, and it has been demonstrated that numerous degradations appear rapidly at different interfaces within the device. Exposure to the outside air, moisture, high temperatures and UV radiation can directly cause these degradations. Intrinsic stability pertains to devices' structural and chemical stability under various photovoltaic operating conditions, even in the presence of pollutants, including oxygen and water, that were incorporated during the device's fabrication. Extrinsic stability focuses on the deficiencies of sealing and moisture-blocking layers. Under typical conditions, degradation processes are triggered or expedited.[91]

6.1 Effect of moisture

Moisture is a significant factor that leads to the decomposition of a perovskite during its synthesis in the surrounding air (Fig. 4a and b–b").[92] Firstly, Frost *et al.* reported the degradation process of the $CH_3NH_3PbI_3$ perovskite in the presence of moisture.[93] Essentially, it comprises the subsequent stages: (a) the reaction between water (H_2O) and the $MAPbI_3$ layer in the devices leads to the formation of CH_3NH_3I and PbI_2; (b) as a result of its unstable condition, CH_3NH_3I undergoes decomposition into CH_3NH_2 and HI. During this stage, the combination of O_2 and UV light readily triggers a reaction with HI (c and d), resulting in the complete breakdown of the $CH_3NH_3PbI_3$ perovskite (eqn (1)–(4)).[94]

$$CH_3NH_3PbI_3 \rightarrow CH_3NH_3I(aq) + PbI_2(s) \quad (1)$$

$$CH_3NH_3I(aq) \rightarrow CH_3NH_3(aq) + HI(s) \quad (2)$$

$$4HI(aq) \rightarrow 2I(s) + 2H_2O \quad (3)$$

$$2HI(aq) \rightarrow I_2(s) + H_2 \quad (4)$$

6.2 Effect of heat

$MAPbI_3$ is inherently unstable when exposed to heat, causing the release of I_2 and the formation of metallic Pb at temperatures as low as 40 °C (similar to the conditions under which the device operates) in the absence of light (eqn (5) and (6)).[95] The decomposition processes is represented in Fig. 4(d).

$$CH_3NH_3PbI_3 \rightarrow CH_3NH_3I + PbI_2 \quad (5)$$

$$PbI_2 \rightarrow Pb0 + I_2 \quad (6)$$

At 80–85 °C temperature, MAI decomposed into more volatile molecules, as shown by the reaction mechanism (eqn (7) and (8)).[96,97]

$$CH_3NH_3I \rightarrow CH_3I + NH_3 \quad (7)$$

$$CH_3NH_3I \rightarrow CH_3NH_2 + HI \quad (8)$$

The reactions described above are feasible. Reaction (7) is thermodynamically more favourable, with an energy difference of around 13–14 kcal mol^{-1} compared to reaction (8). However, reaction (7) also needs a higher activation energy due to the more significant number of bonds that need to be broken while transitioning from the solid to the gas phase. Thus, in most

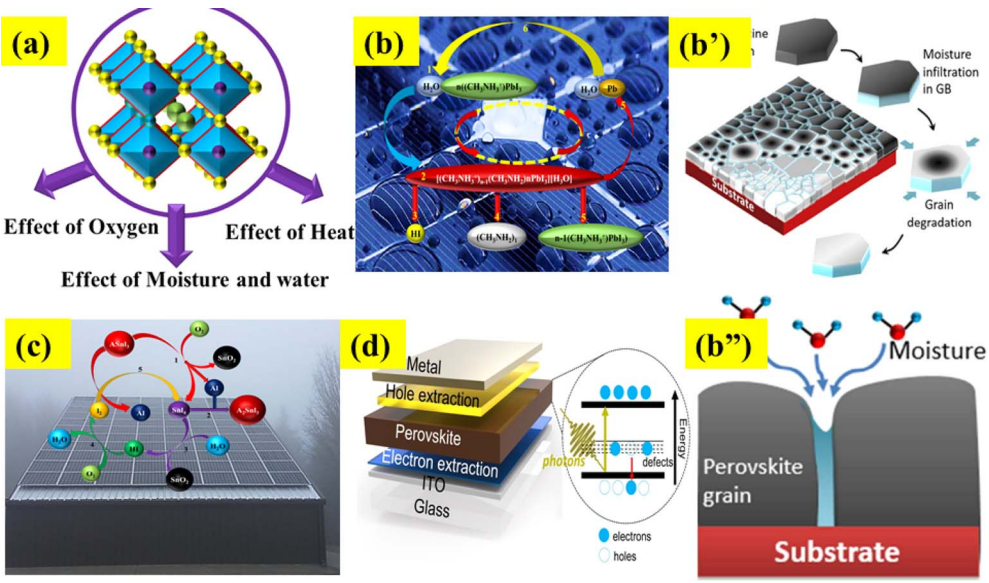

Fig. 4 (a) External factor effect on the stability of PSCs, (b–b") effect of water and moisture. Reproduced with permission.[114] Copyright 2015, American Chemical Society. (c) Influence of oxygen and (d) analysis of the heat effect.

instances, the resulting products that are seen are CH_3NH_2 and HI.[98]

6.3 Effect of oxygen

The perovskite material, *i.e.* $MAPbI_3$, undergoes rapid degradation in the presence of oxygen due to the reaction between MA^+ and oxygen, forming charge barriers. This leads to the accumulation of trapped charges together with electronic traps and mobile defects.[99] An abundance of trapped charges is stored in the perovskite film and triggers the generation of new charges to establish a state of neutrality.[100] This process reduces the efficiency of charge extraction and promotes the recombination of excitons. In the presence of oxygen, $MAPbI_3$ can facilitate the creation of Pb–O bonds, leading to further deterioration of the perovskite.

Furthermore, the presence of oxygen and light expedites the deterioration of the perovskite.[101] In the absence of light, oxygen can combine with $MAPbI_3$ to create I_2, H_2O, CH_3NH_2 and PbI_2. However, this degradation process is undesirable (eqn (9)–(11)).[102,103] The reaction between oxygen and $MAPbI_3$ improves when exposed to light. Due to the movement of electrons, $O_2^{\bullet-}$ reacts with photo-oxidized $MAPbI_3$ and produces the same products without light (eqn (12)–(14)).[104]

$$MAPbI_3 \leftrightarrow CH_3NH_3I + PbI_2 \quad (9)$$

$$MAI \leftrightarrow CH_3NH_2 + HI \quad (10)$$

$$4HI + O_2 \leftrightarrow 2I_2 + 2H_2O \quad (11)$$

$$MAPbI_3 \leftrightarrow MAPbI_3^* \quad (12)$$

$$O_2 \leftrightarrow O_2^{\bullet-} \quad (13)$$

$$MAPbI_3 + O_2^{\bullet-} \leftrightarrow CH_3NH_2 + PbI_2 + 1/2I_2 + H_2O \quad (14)$$

When $MAPbI_3$ reacts with oxygen, whether it is subjected to light or not, it undergoes significant deterioration, which poses a barrier to improving its stability. Hence, it is imperative to limit the oxygen breakdown of the perovskite to achieve high stability for PSCs. Furthermore, $MAPbBr_3$, which is the equivalent of $MAPbI_3$, also experiences deterioration when exposed to oxygen. The process of oxygen degradation in $MAPbBr_3$ remarkably resembles that of $MAPbI_3$ (eqn (15)–(17)).[105,106]

$$MAPbBr_3 \leftrightarrow MABr + PbBr_2 \quad (15)$$

$$MABr \leftrightarrow CH_3NH_2 + HBr \quad (16)$$

$$PbBr_2 + O_2 \leftrightarrow PbO_2 + Br_2 \quad (17)$$

Sn-based PSCs have evolved at a lower rate, primarily due to their inadequate stabilization under changing environmental conditions. Sn-based perovskite materials have poor optical stability because of the rapid oxidation of Sn^{2+} into Sn^{4+}, which demonstrates the self-doping that causes deterioration.[107] Charge-carrier recombination rates of monomolecular and bimolecular substantially affect the efficiency of PSC; however, the charge recombination rate is very small in the order of tens to hundreds of nanoseconds, which may result in poor optical efficiency and stability.[108] Additionally, various solutions were investigated to solve these difficulties, including using SnX_2 additives to reduce the effect of self-doping. The efficiency and stability of Sn-based PSCs have been compared with the Pb-based PSCs. Changes in electronic characteristics such as charge mobility, conductivity, diffusion length, and band alignment occur due to the breakdown of the $FASnI_3$ and $MASnI_3$.[109] The role of the SnI_4-based degradation mechanisms of $(PEA)_{0.2}(FA)_{0.8}SnI_3$ films has been investigated, and SnI_4 in the film easily and quickly emerged to generate I_2 through a two-step method in which the iodine (I) hydrolysis reaction of SnI_4 with H_2O yielded HI and HI oxidation by O_2 yielded I_2. The optical cell degrades fast when I_2 is exposed to $ASnI_3$ resulting in the manufacture of additional SnI_4 generating a cyclic degradation process as represented in Fig. 4(c),[110]

$$2ASnI_3 + O_2 \rightarrow SnI_4 + SnO_2 + 2AI \quad (18)$$

$$SnI_4 + 2AI \rightarrow A_2SnI_6 \quad (19)$$

$$SnI_4 + 2H_2O \rightarrow 4HI + SnO_2 \quad (20)$$

$$4HI + O_2 \rightarrow 2I_2 + 2H_2O \quad (21)$$

$$I_2 + ASnI_3 \rightarrow AI + SnI_4 \quad (22)$$

Two and three-dimensional tin-based perovskite films on $(PEA)_{0.2}(FA)_{0.8}SnI_3$ were investigated for their degradation mechanisms. When moisture and oxygen are mixed with the tin-based perovskite SC, the formation of iodine is speedy. Besides, iodine is an extremely aggressive species that could further react with oxygen in the perovskite to form more SnI_4, which tends to result in a cyclic degradation process in the perovskite structure.[110]

6.4 Effect of raw materials

Efficiency is a cornerstone consideration in PSC design, with the choice of raw materials directly influencing the cell's ability to convert sunlight into electricity. Perovskite absorber materials, such as methylammonium lead iodide ($CH_3NH_3PbI_3$), dictate the light spectrum they can absorb and how effectively they convert it into electrical energy. Additionally, the purity and crystallinity of these materials are paramount, as defects or impurities can hinder charge transport and reduce overall efficiency. Furthermore, selecting hole-transporting and electron-transporting materials, such as spiro-OMeTAD and PCBM, respectively, plays a critical role in facilitating efficient charge extraction and transport within the cell. Stability is another pivotal factor influenced by raw materials in PSCs.[111] Perovskite materials are inherently sensitive to moisture, heat, and light, which can degrade their performance over time. Thus, choosing raw materials, including encapsulation materials and interface layers, is crucial in mitigating degradation mechanisms and ensuring long-term stability. Improvements in material formulations and encapsulation techniques are continuously

sought to enhance the stability and durability of PSCs, enabling their deployment in a wide range of environmental conditions. Cost considerations are paramount in the commercialization of PSCs, with the affordability and availability of raw materials playing a significant role in determining the economic feasibility of large-scale production. While perovskite materials are relatively inexpensive compared to traditional silicon-based SCs, the cost of auxiliary materials, such as hole-transporting layers and electrodes, can add up. Innovations in material synthesis, processing techniques, and supply chain management are essential in driving down production costs and improving the cost competitiveness of PSCs in the renewable energy market.[112] Environmental impact is a growing concern associated with using certain raw materials in PSCs. Lead-based perovskite materials, for instance, cause significant environmental and health problems due to their toxicity and potential for leaching into the environment. Efforts to develop lead-free or low-toxicity alternatives are underway to mitigate these risks and ensure the sustainability of PSC technologies. In summary, the effects of raw materials in PSCs are multifaceted, encompassing efficiency, stability, cost, and environmental impact. By carefully selecting and optimizing raw materials, researchers and manufacturers can develop PSCs that offer high performance, long-term durability, and environmental sustainability, thereby contributing to the widespread adoption of renewable energy technologies.[113]

6.5 Internal heat

Internal factors include the formation of heat caused by the recombination of tail states and the thermalization of charge carriers produced by the absorption of photons with energy higher than the band gap. The active layer of PSCs absorbs photons with higher energy levels than the band gap to generate free electrons and holes. Before reaching the electrodes and generating electricity, these charge carriers may undergo radiative and non-radiative recombination.[115] The internal heat sources can be attributed to energy dissipation resulting from non-radiative recombination at the boundaries between grains and trap-assisted recombination at the interfaces between the layers responsible for charge transport and the perovskite active materials. The thermalization of high-energy charge carriers also generates heat.[116,117] Many types of heating are produced in SCs, including Joule and Peltier heating. Joule heating is an internal heat source when an electrical current passes through a resistive medium.[118] Peltier heating refers to the dissipation of heat at the interface between the metal and semiconductor and is an additional factor that contributes to the formation of internal heat and impacts the performance of the cells.[119,120] Because the internal heat suffers from a wide range of intrinsic defects reproduced, including atomic vacancy, interstitials and wider dimensionality imperfections present in perovskite films are a significant element influencing the durability and efficiency of PSCs.[121] Due to internal factors, the abnormality shows irregular photocurrent density–voltage (*J*–*V*) hysteresis behavior and low operational stability resulting from inner factors associated with connections of interface contact.[122]

7. Potential lead toxicity

Approximately 50% of perovskite films consist of lead (Pb), which presents a significant hazard to living organisms and the environment.[123–125] Pb poisoning from PSCs can manifest in two stages: during operation and at the end of the life cycle. Although effective waste disposal and recycling can regulate the former issue, the release of lead during the functioning of these solar cells is a significant cause for worry.[126,127] The importance of effective encapsulants cannot be emphasized enough for the secure and environmentally friendly functioning of Pb-containing PSCs. Under typical operational conditions, glass encapsulation is sufficient to contain lead. However, in the event of cracks and fractures in the panel, lead can be released from beneath the perovskite surface.[128–130] The water solubility of Pb^{2+} ions poses a hazardous outcome. To tackle this difficulty, it is necessary to use lead-absorbing materials such as films, tape, or coverings in addition to standard encapsulants. Lead-absorbing materials must effectively manage leaks under challenging environmental conditions, including heavy rains, and keep the lead concentration in water below the 15 μg L^{-1} level set by the United States Environmental Protection Agency (EPA).[131,132]

8. Encapsulation

PSC devices are very vulnerable to degradation when exposed to external atmospheric conditions since the perovskite material tends to disintegrate upon contact with moisture. One way to improve the stability of a PSCs is by encapsulating the device. Device encapsulation will influence PSC commercialization. Devices that lacked encapsulation showed significant deterioration when constantly exposed to light for several hours, whereas encapsulated devices had a longer lifespan.[133,134] The encapsulation technique entails using a moisture and oxygen-impermeable substance to encapsulate the device, along with inserting an electrode strip that can be attainable with no damage to the integrity of the insulating encapsulation.[135,136]

8.1 Encapsulation technique with improved stability

Extensive research has been conducted in photovoltaics to evaluate the efficacy of different encapsulation methods. This research is motivated by the need to address the degradation issue, which significantly impacts the stability of SCs. An encapsulating technique with enhanced stability derived from organic light emitting diode (OLED) technology involves using a cover glass lid, UV epoxy sealing, and a desiccant.[137] It was demonstrated that partial encapsulation, which permits direct contact with the electrodes, leads to moisture leaking at the edges and consequently reduces the lifespan relative to complete encapsulation with shielded edges.[138] Undoubtedly, meticulous encapsulation can greatly prolong the lifespans of devices. Krebs *et al.* devised a technique for manufacturing polymer solar cells using a fully roll-to-roll method.[139] The straightforward encapsulation somewhat enhanced the stability of the device. Tanenbaum *et al.* enhanced this method by

sealing the edges, leading to much-enhanced device stability. Single-layer thin films are appealing due to the straightforwardness of the fabrication technique.[140] Multilayer films are commonly employed for encapsulating organic photovoltaic systems, typically including successive layers of organic or inorganic materials.[141]

Regarding encapsulation architecture, the Russian doll architecture is employed.[142] A practical approach to encapsulation involves a two-stage process. First, low-temperature (<100 °C) treatment of materials is carried out after a second sealing stage at an elevated temperature (130 °C). This method has been proven to improve device performance.[143] Hwang *et al.* demonstrated the ability to enhance the operational lifespan of a device by applying a coating of amorphous Teflon through a spinning process. Chang *et al.* employed the notion of a compact alumina layer as a preserving shield. They demonstrated that the atomic layer deposition of an Al_2O_3 layer greatly enhanced the resistance to air degradation.[144] Anta and colleagues studied a straightforward technique for encapsulating perovskite solar cells without using solvents. They used a thin film made of plasma polymer that adheres well to the cells. The researchers found that this method significantly enhanced the stability of the devices, not only when exposed to moisture and light but also when subjected to humid air and even submerged in water.[145]

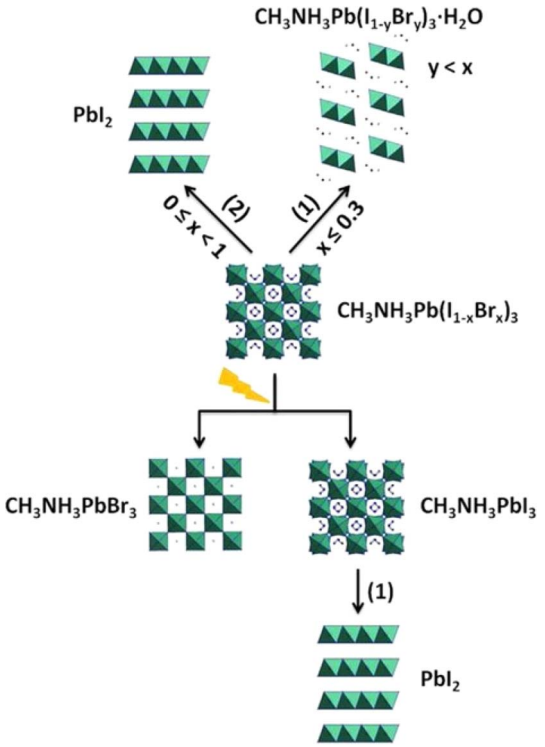

Fig. 5 Diagram of degradation of $MAPb(I_{1-x}Br_x)_3$ exposed to humidity.[151]

9. Strategies to improve stability

$CH_3NH_3PbI_3$ is the most often utilized perovskite substance. Deviation from this traditional framework could potentially result in enhanced environmental stability. Noh *et al.* adjusted the chemical composition of $CH_3NH_3Pb(I_{1-x}Br_x)_3$ perovskites by replacing iodine ions with bromine ions.[146] Devices without encapsulation, using $MAPb(I_{1-x}Br_x)_3$ ($x = 0$, 0.06, 0.20, 0.29), were kept in an environment with 35% humidity at the ambient temperature for twenty days. The humidity rose to 55% on day four. For $x = 0$ and 0.06, PCEs declined significantly following humidity shock, while $x = 0.20$ and 0.29 exhibited steady PCEs for 20 days.[2,147] Ruess *et al.* used XRD and EDS to study the impact of partial Br substitution for I in $MAPbI_3$ on stability in the dark and under light (room temperature, 67 ± 5% RH).[148] As Br content increased, PbI_2 production was suppressed and the monohydrate phase occurred. $MAPb(I_{1-x}Br_x)_3$ with low Br content stored under dark and humid conditions formed a monohydrate, while those with high Br content demonstrated good moisture resistance and prevented hydrate formation. Br content was substantially lower in $MAPb(I_{1-y}Br_y)_3 \cdot H_2O$ than $MAPb(I_{1-x}Br_x)_3$, suggesting Br diffusion during monohydrate formation. As Br concentration declined, PbI_2 content increased with monohydrate formation, whereas $MAPbBr_3$ had no PbI_2.[149]

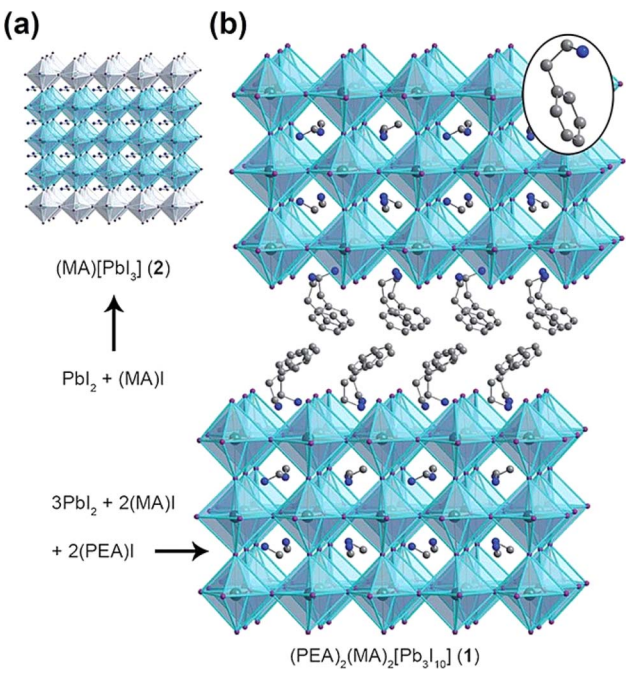

Fig. 6 Crystal structures of (a) 3D perovskite MAPbI and (b) 2D perovskite $PEA_2MA_2Pb_3I_{10}$.[153]

$$n[MAPb(I_{1-x}Br_x)_3] + H_2O \rightarrow (n-1)[MAPb(I_{1-z}Br_z)_3] + [MAPb(I_{1-y}Br_y)_3] \cdot H_2O$$

where $z = (nx - y)/(n - 1)$,and

$$n[MAPb(I_{1-x}Br_x)_3] \rightarrow (n-1)\,[MAPb(I_{1-z}Br_z)_3] + PbI_2 + CH_3NH_2 + HI$$

where $z = nx/(n-1)$.

The improved stability achieved by utilizing Br can be due to the improved hydrogen bonding between the NH_3^+ group and the halide ions. This interaction is believed to stabilize the framework that consists of corner-sharing (PbI_6) octahedra.[150] When exposed to light, the $MAPb(I_{1-x}Br_x)_3$ material experienced halide segregation, which prevented the partial replacement from enhancing stability and resulted in the formation of PbI_2. A potential breakdown pathway for $MAPb(I_{1-x}Br_x)_3$ is presented in Fig. 5.

The device utilized the layered composition of $(PEA)_2(MA)_2[Pb_3I_{10}]$ [PEA = $C_6H_5(CH_2)_2NH_3^+$] to enhance its resistance to moisture. The crystal structure of $(PEA)_2(MA)_2[Pb_3I_{10}]$ is depicted in Fig. 6, illustrating the separation of the 3D $MAPbI_3$ domain by the PEA chain.[152] Despite having a higher bandgap of 2.1 eV, the perovskite-based device with a layered structure exhibited a significantly lower photocurrent of 6.72 mA cm^{-2}. However, it demonstrated improved stability due to the better chemical bonding between Pb and I atoms resulting from the reduction in dimensionality. Under the conditions of being exposed to ambient air with a relative humidity of 52% at room temperature, the compound $(PEA)_2(MA)_2[Pb_3I_{10}]$ exhibited remarkable stability against moisture for 46 days. In contrast, the $MAPbI_3$ film dissolved into PbI_2 after 4 days.[152]

In addition to stability challenges, the perovskites that are most frequently employed and include Pb halides also encounter another obstacle to becoming commercially viable, which is the toxicity risks associated with lead. Tin (Sn) is the most suitable substitute for Pb because it is a group 14 metal with four electrons in its outer shell. The enlargement of group 14 elements results in decreased stability of the +2 oxidation state, leading to notable stability issues for perovskites that contain Sn.[154] Multiple research teams have fabricated and analyzed solar cells that include $CH_3NH_3SnI_3$ as the perovskite absorber. Noel *et al.* fabricated a device by applying a thin layer of $CH_3NH_3SnI_3$ onto a TiO_2 substrate using the spin coating technique. Because of the instability of the Sn perovskite, all manufacturing was carried out in a glovebox filled with nitrogen. Immediately after removing an unenclosed film from the glovebox, a loss of color was seen.[154] The authors propose that the rapid oxidation occurring under normal conditions results from the oxidation of the Sn^{2+} ions, leading to the disintegration of the perovskite structure. As a result, the reaction produces tin oxides and MAI. Furthermore, it was revealed that enclosed electronics, when evaluated under ambient conditions, likewise exhibited rapid degradation. This could be attributed to the infiltration of oxygen or moisture at the metal connections.

To conduct additional stability testing, the $CH_3NH_3SnI_3$ film was encapsulated and hermetically sealed using an epoxy resin. For four months, the sample was kept in a glovebox filled with nitrogen and subjected to continuous exposure to light at an intensity of 76 mW cm^{-2}. No noticeable fading of color was observed. In addition to stability issues, scientists have observed that the diffusion duration of Sn-based perovskites is considerably shorter compared to their Pb-based counterparts. While more than 6% PCE was attained, the limited diffusion length might impede the production of devices with a flat structure. It may be necessary to incorporate a mixed heterojunction layer similar to that used in organic photovoltaic (OPV) devices. Hao *et al.* simultaneously reported the incorporation of Sn halides in perovskite solar cells. In addition to $CH_3NH_3SnI_3$, the halide's chemical makeup was modified by introducing $Br(CH_3NH_3Sn(I_{3-x}Br_x))$. A perovskite material, namely $CH_3NH_3Sn(IBr_2)$, attained an efficiency of about 6%.[154–156]

10. Replacement of lead by heterovalent and isovalent elements

Recently, Pb-based PSCs have attained 25.2% PCE because of their significant absorption coefficient, extensive diffusion length, and low defect density.[157] Furthermore, these technologies' widespread applications and commercialization are significantly hindered by the inclusion of poisonous Pb. The better PV capabilities of the Pb-based halide perovskites have been assigned to the perovskite structure and the inactive Pb 6s orbitals. It has been demonstrated that various cations, like Ge^{2+}, Sn^{2+}, Sb^{3+}, Bi^{3+}, and Cu^{2+}, may substitute Pb to generate Pb-free PSCs. Pb-free PSCs have become more desirable due to the growing need for nontoxic elements in photocatalytic absorbers.[158]

10.1 Sn-based PSCs

Sn-based PSCs are considered potentially valuable alternatives because of their lower toxicity and superior optoelectronic features.[159,160] Moreover, their lower optical E_g (1.2–1.4 eV) is nearer to the ideal value as reflected by the Shockley–Queisser limit (1.34 eV), making Sn-based PSCs more suited light absorbers for SCs and other optoelectronic devices functioning in the near IR region, including photodetectors and LEDs.[161] This is because the optimum value is 1.34 eV. Despite this, Sn-based SCs have not yet achieved a high potential level compared to Pb-based PSCs due to the large oxidative power of Sn^{2+} to form Sn^{4+}, which promoted accidental self-p-doping in Sn-based PSCs. This, in turn, causes the shortening of SC devices even in gloveboxes packed with nitrogen. As a result, significant work has been put into minimizing the impact of oxidation on Sn.[162] In recent years, several effective methods have been investigated to enhance the working of Sn-based PSCs. These methods include (1) the employment of halide or cation Sn-based PSCs,[163] (2) the addition of a successive deposition route, and (3) the production of quasi-2D Sn-based photovoltaic SCs. The structural alteration of 3D Sn-based PSCs into quasi-2D PSCs by inserting a hydrophobic large alkyl chain cation has yielded notable increases in device working efficiency and stability.[164] This was accomplished by changing the structure of the PSCs from 3D to quasi-two-dimensional. S. Shao *et al.* claimed a PCE as large as 9% for Sn-based PSCs synthesized using the spin coating process for the first time in 2018. A V_{oc} of 0.525 V, J_{sc} of 24.1 mA cm^{-2} and an FF of 0.71 have been displayed by this 2D/3D device.[165] The $FA_{0.75}MA_{0.25}SnI_3$-based PSCs were prepared using the gas pump treatment technology. They attained an impressive efficiency of 1.85%, which is the most

Table 1 Sn-based PSCs with different preparation methods and V_{oc}, J_{sc}, FF and PCE

Sn-based PSCs	Preparation method	Absorber morphology	PSC structure	V_{oc} (V)	J_{sc} (mA cm^{-2})	FF (%)	PCE (%)	Ref.
Sn-based hybrid PSCs 2018	Single step spin coating method	$FASnI_3$ 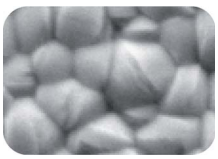	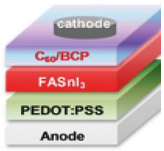	0.525	24.1	71	9	165
Sn-based PSCs 2018	Gas pump treatment	$FA_{0.75}MA_{0.25}SnI_3$ 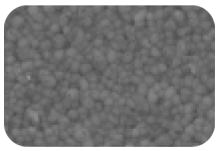	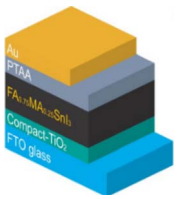	0.26	17.4	42	1.85	166
Sn-based hybrid PSCs 2018	One-step method	$FA_{0.75}MA_{0.25}SnI_3$ 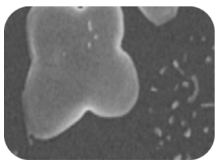	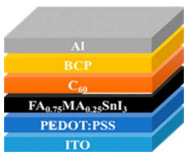	0.55	24.3	67.3	9.06	167
Sn-based PSCs 2018	—	$FASnI_3$-$EDAI_2$ 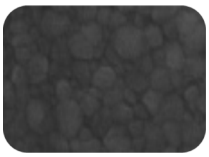	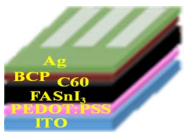	0.583	21.3	0.718	8.9	168
Sn-based PSCs 2019	Ultra-sonication	$FASnI_3 + NH_4H_2PO_2$ 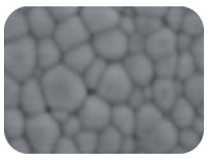		0.55	19.39	68.8	7.3	169
Sn-based PSCs 2019	Two-step method	$FASnI_3$ + BDT 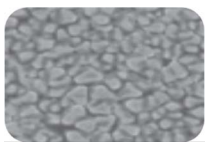	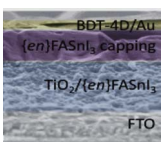	0.497	22.41	68.21	7.59	170
Sn-based PSCs 2019	—	$FASnI_3$ + PVA 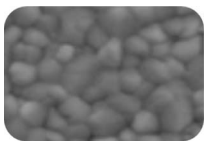	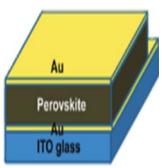	0.632	20.37	0.686	8.9	171
Sn-based PSCs 2020	Ultra-sonication	$FASnI_3$ + TBA	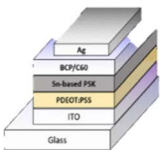	0.51	19.7	69.6	7	172

Table 1 (*Contd.*)

Sn-based PSCs	Preparation method	Absorber morphology	PSC structure	V_{oc} (V)	J_{sc} (mA cm^{-2})	FF (%)	PCE (%)	Ref.
Sn-based PSCs 2020	One-step method	$FASnI_3$ + π-conjugated base 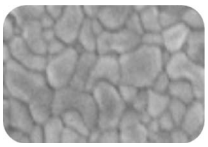	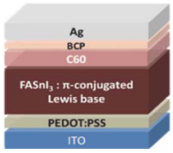	0.63	—	74.7	10.1	173
Sn-based PSCs 2020	Spin coating	$FASnI_3$ 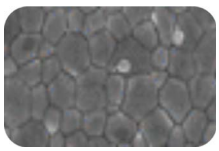	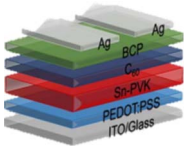	0.69	21.53	68.46	10.17	174
Sn-based PSCs 2021	Ultra-sonication	$FA_{0.75}MA_{0.25}SnI_{2.75}Br_{0.25}$ 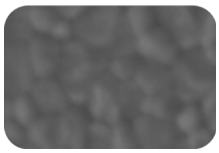		0.52	22.3	0.69	8.07	175
Sn-based PSCs 2022	Spin coating	$FA_{0.98}EDA_{0.01}SnI_3$ + Me_3SiX 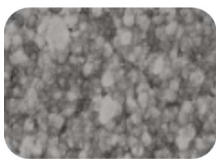	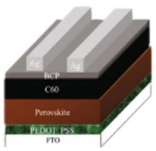	0.70	24.11	72	12.22	176

considerable efficiency reported for Sn-based devices with the arrangement of FTO/c-TiO_2/perovskite/HTM/electrode.[166] All the above discussions based on Sn are represented in Table 1.

10.2 Ge-based PSCs

A further element that is a compelling possibility for PSCs is Ge, which, like Sn and Pb, is an element that belongs to group 14. In contrast to Pb^{2+}, Ge^{2+} possesses a stronger electronegativity, a high covalent nature, and an ionic radius (73 pm) lower than the one possessed by Pb^{2+}. In addition, the electronegativity of Ge^{2+} is greater than that of Pb^{2+} (119 pm).[177] The PCE of Ge-based PSCs was raised to 0.57% by replacing 10% of the iodide with bromide.[178] For $CsSn_{0.5}Ge_{0.5}I_3$-based PSCs a PCE of 7.03% has been achieved *via* a solid-state reaction with V_{oc}, J_{sc} and FF measured to be 0.63 V, 18.61 mA cm^{-2}, and 60.6%, respectively.[179] The discussions of Ge-based perovskites are reported in Table 2.

10.3 Sb-based PSCs

Fabricating a novel set of perovskite-like compounds has generated a structure similar to perovskites with the formula $A_3B_2X_9$, where A is a monovalent and B is a trivalent cation. These perovskite-like compounds were fabricated *via* the heterogeneous replacement of Pb with trivalent cations (for example, Bi and Sb). These systems may also be described by the formula $AB_{2/3}X_3$, which states that to preserve charge neutrality, one out of every three octahedral sites occupied by B^{3+} must remain empty.[186] The various factors that affect the PCE of Sb-based PSCs are illustrated in Table 3.

10.4 Bi-based PSCs

Many research groups are interested in Bi-based halide PSCs, which have the chemical formula $A_3Bi_2X_9$ (where A refers to a monovalent cation, such as Na^+, K^+, Rb^+, Cs^+, and $CH_3NH_3^+$, and X refers to a halogen atom). Bi-based halide perovskites solve Pb-based PSCs' stability and toxicity problems.[195] $Cs_3Bi_2I_9$ PSCs have been synthesized by the dissolution–recrystallization method and attained a PCE of 3.20% and FF of 64.38%.[195] A PCE of 1.26% was achieved by the Bi-based halide ($Cs_3Bi_2I_{10}$) PSCs using the solution process approach.[196] The PCE, FF, J_{sc} and V_{oc} for $Cs_2AgBiBr_6$-based PSCs were found to be 1.16%, 43.9%, 2.83 mA cm^{-2} and 0.94 V, respectively.[197] The Bi-based perovskite discussion is represented in Table 4.

Table 2 Different methods for synthesis of Ge-based PSCs and their V_{oc}, J_{sc}, FF and PCE

Ge-based PSCs	Preparation method	Absorber morphology	PSC structure	V_{oc} (V)	J_{sc} (mA cm^{-2})	FF (%)	PCE (%)	Ref.
Ge-based PSCs 2018	Spin coating	$MAGeI_{2.7}Br_{0.3}$ 	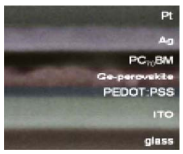	0.46	2.43	51	0.57	178
Ge-based PSCs 2019	Solid state reaction	$CsSn_{0.5}Ge_{0.5}I_3$ 	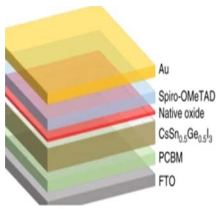	0.63	18.61	60.6	7.03	179
Ge-based PSCs 2019	—	$CsSnGeI_3$	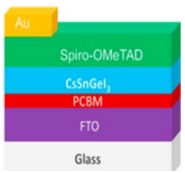	0.797	20.43	81.63	13.29	180
Ge-based PSCs 2021	Simulation methodology	$CsGeI_3$	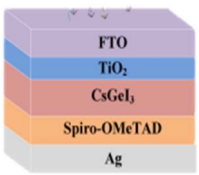	1.04	23.31	75.46	18.30	181
Ge-based PSCs 2021	—	$CsSn_{0.5}Ge_{0.5}I_3$	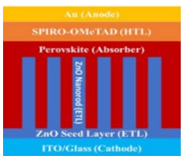	0.97	29.56	84.15	21.27	182
Ge-based PSCs 2021	Solution processed method	$CH_3NH_3GeI_3$	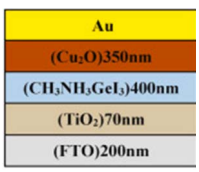	1.00v	25.75	79.21	20.52	183
Ge based PSCs 2022	Simulation methodology	$CH_3NH_3GeI_3$	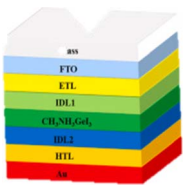	1.264	12.20	85.46	13.18	184
Ge-based PSCs 2022	Numerical simulation	$CsGeI_3$	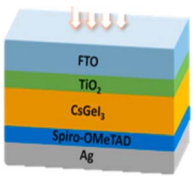	0.667	22.08	73.49	10.8	185

Table 3 Sb-based PSCs with different synthesis methods and their V_{oc}, J_{sc}, FF and PCE

Sb-based PSCs	Preparation method	Absorber morphology	PSC structure	V_{oc} (V)	J_{sc} (mA cm^{-2})	FF (%)	PCE (%)	Ref.
Sb-based PSCs 2018	Spin coating	$(CH_3NH_3)_3Sb_2Cl_XI_{9-X}$ 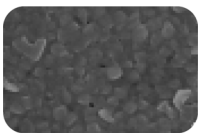	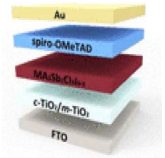	0.70	4.74	59	1.96	187
Sb-based PSCs 2018	Spin coating	$(CH_3NH_3)_3Sb_2I_9$ 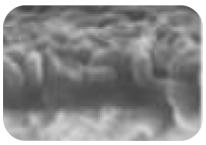		0.70	6.64	59.60	2.77	188
Sb-based PSCs 2018	Solution-processed method	$Cs_3Sb_2I_9$ 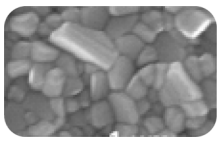		0.72	5.31	38.97	1.49	189
Sb-based PSCs 2020	Lewis-pair mediation	$Cs_3Sb_2I_9$	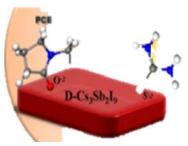	0.79	3.76	54	1.86	190
Sb-based PSCs 2020	Simple hot-injection method	$Cu_{12}Sb_4S_{13}$ 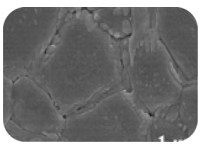	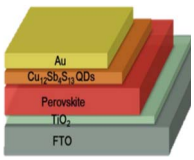	1.05	21.85	61.60	14.13	191
Sb-based PSCs 2021	—	$Cs_3Sb_2I_9$ 	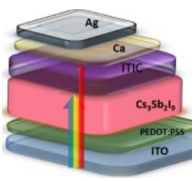	0.74	47.7	22.4	9.2	192
Sb-based PSCs 2022	Spin coating	$Cs_3Sb_2I_{9-x}Cl_x$ 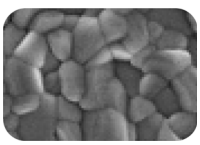	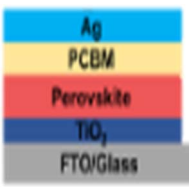	0.65	6.77	50.3	2.22	193
Sb-based PSCs 2022	Simulation methodology	$Cs_3Sb_2I_9$ 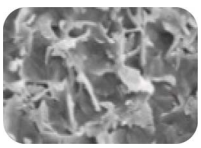	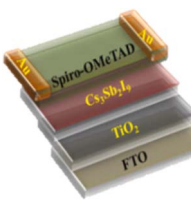	1.32	13.13	72.01	12.54	194

Table 4 Bi-based PSCs with different synthesis methods and their V_{oc}, J_{sc}, FF and PCE

Bi-based PSCs	Preparation method	Absorber morphology	PSC structure	V_{oc} (V)	J_{sc} (mA cm^{-2})	FF (%)	PCE (%)	Ref.
Bi-based PSCS 2018	Dissolution–recrystallization process	$Cs_3Bi_2I_9$ 	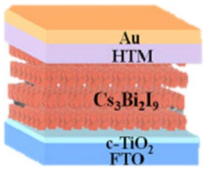	0.86	5.78	64.38	3.20	195
Bi-based PSCs 2019	Solvent annealing	$Cs_3Bi_2I_{10}$ 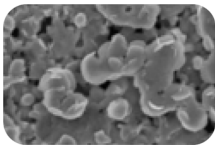	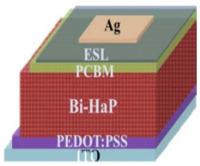	0.74	3.42	51	1.26	196
Bi-based PSCs 2020	Ultrasonic treatment	$Cs_3Bi_2I_9$–$Ag_3Bi_2I_9$ 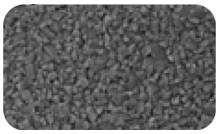	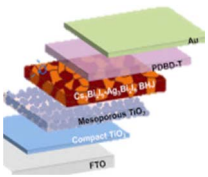	0.78	7.65	60.12	3.59	198
Bi-based PSCs 2021	One-step spin coating	$Cs_2AgBiBr_6$ 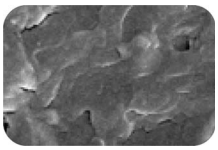	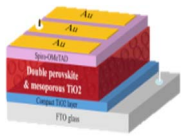	0.94	2.83	43.9	1.16	197

11. Conclusion and outlook

Climate change and environmental damage have prompted the development of much more environmentally sustainable and cost-effective alternatives to fossil fuels. Lead PSCs have been less expensive than traditional technologies, with a remarkable increase in efficiency in a short period, with their PCE rising from 3.8% to 25.2% in eleven years. Despite their remarkable electronic and optical characteristics, certain impediments, such as the dependence on toxic lead and inadequate stability, hinder their extensive commercial viability. As a result, researchers have directed their efforts towards substituting lead with less hazardous compounds, all the while striving to uphold the efficiency and stability of PSCs. Numerous Pb-free PSCs, such as Sn-based, Ge-based, Bi-based, and Sb-based PSCs, have made significant progress, reaching approximately 12.22, 21.27, 3.59, and 12.54% PCE, respectively. In addition, they had significant issues associated with the degradation caused by moisture. The perovskite structure has high electrical and optical characteristics to achieve high efficiency. In addition, encapsulation technologies have been developed to improve the PSC stability and reduce lead leakage. A cost-effective and efficient encapsulation approach for rigid and flexible perovskite SCs and modules is combining commercially available cation exchange resin with widely used UV resins. The release of Pb^{2+} is attributed to perovskite damage that contaminates the environment and threatens human health. From the deteriorated perovskite PV devices, more than 90% of the Pb^{2+} PSCs were more stable when an Al_2O_3 layer of 50 nm thickness was placed on top of them as an encapsulant. The suitable temperature environment has shown a supportive effect for PSCs while providing a good moisture barrier. When the PSCs were exposed to damp heat for 72 hours at 45 °C, the encapsulated perovskite devices performed admirably as moisture barriers. The solution-based multilayer encapsulation of flexible solar modules and other optoelectronic devices, such as light-emitting devices and photodetectors, has been established to enable reliable, scalable, and easy encapsulation for future large-area PSCs.

Conflicts of interest

There are no conflicts to declare.

Acknowledgements

Authors are grateful to the Pakistan Science Foundation, Islamabad, Pakistan through project PSF/CRP/P-GCU/Consrm-92 (Muhammad Ikram PI).

References

1 I. Khan, L. Han, H. Khan and L. T. Kim Oanh, Analyzing Renewable and Nonrenewable Energy Sources for Environmental Quality: Dynamic Investigation in

Developing Countries, *Math. Probl. Eng.*, 2021, **2021**, 1–12, DOI: 10.1155/2021/3399049.

2 S. A. Raza and N. Shah, *Impact of Financial Development, Economic Growth and Energy Consumption On Environmental Degradation: Evidence from Pakistan, Munich Pers*, RePEc Arch, 2018, pp. 1–26, https://bbejournal.com/index.php/BBE/article/download/184/142.

3 N. R. Moheimani and D. Parlevliet, Sustainable solar energy conversion to chemical and electrical energy, *Renewable Sustainable Energy Rev.*, 2013, **27**, 494–504, DOI: 10.1016/j.rser.2013.07.006.

4 D. Lau, N. Song, C. Hall, Y. Jiang, S. Lim, I. Perez-Wurfl, Z. Ouyang and A. Lennon, Hybrid solar energy harvesting and storage devices: the promises and challenges, *Mater. Today Energy*, 2019, **13**, 22–44, DOI: 10.1016/j.mtener.2019.04.003.

5 Y. Liang and L. Yu, Development of semiconducting polymers for solar energy harvesting, *Polym. Rev.*, 2010, **50**, 454–473, DOI: 10.1080/15583724.2010.515765.

6 H. Abdy, A. Aletayeb, M. Bashirpour, Z. Heydari, M. Kolahdouz, E. Asl-Soleimani, Z. Kolahdouz and G. Zhang, Synthesis, optical characterization, and simulation of organo-metal halide perovskite materials, *Opt.*, 2019, **191**, 100–108, DOI: 10.1016/j.ijleo.2019.06.007.

7 E. H. Jung, N. J. Jeon, E. Y. Park, C. S. Moon, T. J. Shin, T. Y. Yang, J. H. Noh and J. Seo, Efficient, stable and scalable perovskite solar cells using poly(3-hexylthiophene), *Nature*, 2019, **567**, 511–515, DOI: 10.1038/s41586-019-1036-3.

8 S. C. Yadav, V. Manjunath, A. Srivastava, R. S. Devan and P. M. Shirage, Stable lead-free Cs4CuSb2Cl12 layered double perovskite solar cells yielding theoretical efficiency close to 30%, *Opt. Mater.*, 2022, **132**, 112676, DOI: 10.1016/j.optmat.2022.112676.

9 H. Su, T. Wu, D. Cui, X. Lin, X. Luo, Y. Wang and L. Han, The Application of Graphene Derivatives in Perovskite Solar Cells, *Small Methods*, 2020, **4**, 2000507, DOI: 10.1002/smtd.202000507.

10 S. Wu, R. Chen, S. Zhang, B. H. Babu, Y. Yue, H. Zhu, Z. Yang, C. Chen, W. Chen, Y. Huang, S. Fang, T. Liu, L. Han and W. Chen, A chemically inert bismuth interlayer enhances long-term stability of inverted perovskite solar cells, *Nat. Commun.*, 2019, **10**, 1161, DOI: 10.1038/s41467-019-09167-0.

11 N. Arora, M. I. Dar, A. Hinderhofer, N. Pellet, F. Schreiber, S. M. Zakeeruddin and M. Grätzel, Perovskite solar cells with CuSCN hole extraction layers yield stabilized efficiencies greater than 20%, *Science*, 2017, **358**, 768–771, DOI: 10.1126/science.aam5655.

12 S. Bai, P. Da, C. Li, Z. Wang, Z. Yuan, F. Fu, M. Kawecki, X. Liu, N. Sakai, J. T. W. Wang, S. Huettner, S. Buecheler, M. Fahlman, F. Gao and H. J. Snaith, Planar perovskite solar cells with long-term stability using ionic liquid additives, *Nature*, 2019, **571**, 245–250, DOI: 10.1038/s41586-019-1357-2.

13 N. Li, S. Tao, Y. Chen, X. Niu, C. K. Onwudinanti, C. Hu, Z. Qiu, Z. Xu, G. Zheng, L. Wang, Y. Zhang, L. Li, H. Liu, Y. Lun, J. Hong, X. Wang, Y. Liu, H. Xie, Y. Gao, Y. Bai, S. Yang, G. Brocks, Q. Chen and H. Zhou, Cation and anion immobilization through chemical bonding enhancement with fluorides for stable halide perovskite solar cells, *Nat. Energy*, 2019, **4**, 408–415, DOI: 10.1038/s41560-019-0382-6.

14 Z. Li, X. Wu, S. Wu, D. Gao, H. Dong, F. Huang, X. Hu, A. K. Y. Jen and Z. Zhu, An effective and economical encapsulation method for trapping lead leakage in rigid and flexible perovskite photovoltaics, *Nano Energy*, 2022, **93**, 106853, DOI: 10.1016/j.nanoen.2021.106853.

15 Y. Du, Q. Tian, J. Huang, Y. Zhao, X. Chang, A. Zhang and S. Wu, Heterovalent Ga3+ doping in solution-processed Cu2ZnSn(S,Se)4 solar cells for better optoelectronic performance, *Sustainable Energy Fuels*, 2020, **4**, 1621–1629, DOI: 10.1039/c9se00705a.

16 E. Y. Choi, J. Kim, S. Lim, E. Han, A. W. Y. Ho-Baillie and N. Park, Enhancing stability for organic-inorganic perovskite solar cells by atomic layer deposited Al2O3 encapsulation, *Sol. Energy Mater. Sol. Cells*, 2018, **188**, 37–45, DOI: 10.1016/j.solmat.2018.08.016.

17 X. Jiang, F. Wang, Q. Wei, H. Li, Y. Shang, W. Zhou, C. Wang, P. Cheng, Q. Chen, L. Chen and Z. Ning, Ultra-high open-circuit voltage of tin perovskite solar cells via an electron transporting layer design, *Nat. Commun.*, 2020, **11**, 1245, DOI: 10.1038/s41467-020-15078-2.

18 S. Cao, H. Wang, H. Li, J. Chen and Z. Zang, Critical role of interface contact modulation in realizing low-temperature fabrication of efficient and stable CsPbIBr2 perovskite solar cells, *Chem. Eng. J.*, 2020, **394**, 124903, DOI: 10.1016/j.cej.2020.124903.

19 T. Ye, Y. Hou, A. Nozariasbmarz, D. Yang, J. Yoon, L. Zheng, K. Wang, K. Wang, S. Ramakrishna and S. Priya, Cost-Effective High-Performance Charge-Carrier-Transport-Layer-Free Perovskite Solar Cells Achieved by Suppressing Ion Migration, *ACS Energy Lett.*, 2021, **6**, 3044–3052, DOI: 10.1021/acsenergylett.1c01186.

20 N. Mondal, A. De and A. Samanta, All-inorganic perovskite nanocrystal assisted extraction of hot electrons and biexcitons from photoexcited CdTe quantum dots, *Nanoscale*, 2018, **10**, 639–645, DOI: 10.1039/c7nr07830g.

21 H. R. Mohseni, M. Dehghanipour, N. Dehghan, F. Tamaddon, M. Ahmadi, M. Sabet and A. Behjat, Enhancement of the photovoltaic performance and the stability of perovskite solar cells via the modification of electron transport layers with reduced graphene oxide/polyaniline composite, *Sol. Energy*, 2021, **213**, 59–66, DOI: 10.1016/j.solener.2020.11.017.

22 J. Xu, R. Saklatvala, S. Mittal, S. Deshmukh and A. Procopio, Recent Progress of Potentiating Immune Checkpoint Blockade with External Stimuli—an Industry Perspective, *Adv. Sci.*, 2020, **7**, 1903394, DOI: 10.1002/advs.201903394.

23 I. Poli, G. W. Kim, E. L. Wong, A. Treglia, G. Folpini and A. Petrozza, High External Photoluminescence Quantum Yield in Tin Halide Perovskite Thin Films, *ACS Energy Lett.*, 2021, **6**, 609–611, DOI: 10.1021/acsenergylett.0c02612.

24 T. Soto-Montero, N. Flores-Diáz, D. Molina, A. Soto-Navarro, A. Lizano-Villalobos, C. Camacho, A. Hagfeldt and L. W. Pineda, Dopant-Free Hole-Transport Materials with Germanium Compounds Bearing Pseudohalide and Chalcogenide Moieties for Perovskite Solar Cells, *Inorg. Chem.*, 2020, **59**, 15154–15166, DOI: 10.1021/acs.inorgchem.0c02120.

25 D. Zhou, T. Zhou, Y. Tian, X. Zhu and Y. Tu, Perovskite-Based Solar Cells: Materials, Methods, and Future Perspectives, *J. Nanomater.*, 2018, **2018**, 1–15, DOI: 10.1155/2018/8148072.

26 A. Husainat, W. Ali, P. Cofie, J. Attia and J. Fuller, Simulation and Analysis of Methylammonium Lead Iodide ($CH_3NH_3PbI_3$) Perovskite Solar Cell with Au Contact Using SCAPS 1D Simulator, *Am. J. Opt. Photonics*, 2019, **7**, 33, DOI: 10.11648/j.ajop.20190702.12.

27 A. B. Coulibaly, S. O. Oyedele, N. R. Kre and B. Aka, Comparative Study of Lead-Free Perovskite Solar Cells Using Different Hole Transporter Materials, *Model. Numer. Simul. Mater. Sci.*, 2019, **9**, 97–107, DOI: 10.4236/mnsms.2019.94006.

28 M. M. Salah, M. Abouelatta, A. Shaker, K. M. Hassan and A. Saeed, A comprehensive simulation study of hybrid halide perovskite solar cell with copper oxide as HTM, *Semicond. Sci. Technol.*, 2019, **34**, 115009, DOI: 10.1088/1361-6641/ab22e1.

29 M. Mehrabian and S. Dalir, 11.73% efficient perovskite heterojunction solar cell simulated by SILVACO ATLAS software, *Opt.*, 2017, **139**, 44–47, DOI: 10.1016/j.ijleo.2017.03.077.

30 L. Lin, T. W. Jones, T. C. J. Yang, N. W. Duffy, J. Li, L. Zhao, B. Chi, X. Wang and G. J. Wilson, Inorganic Electron Transport Materials in Perovskite Solar Cells, *Adv. Funct. Mater.*, 2021, **31**, 2008300, DOI: 10.1002/adfm.202008300.

31 S. Do Sung, D. P. Ojha, J. S. You, J. Lee, J. Kim and W. I. Lee, 50 nm sized spherical TiO2 nanocrystals for highly efficient mesoscopic perovskite solar cells, *Nanoscale*, 2015, **7**, 8898–8906, DOI: 10.1039/c5nr01364j.

32 A. Chilvery, S. Das, P. Guggilla, C. Brantley and A. Sunda-Meya, A perspective on the recent progress in solution-processed methods for highly efficient perovskite solar cells, *Sci. Technol. Adv. Mater.*, 2016, **17**, 650–658, DOI: 10.1080/14686996.2016.1226120.

33 P. Würfel, *Physics of Solar Cells: From Principles to New Concepts*, John Wiley and Sons, 2007, DOI: 10.1002/9783527618545.

34 N. Suresh Kumar and K. Chandra Babu Naidu, A review on perovskite solar cells (PSCs), materials and applications, *J. Mater.*, 2021, **7**, 940–956, DOI: 10.1016/j.jmat.2021.04.002.

35 D. M. Chapin, C. S. Fuller and G. L. Pearson, A new silicon p–n junction photocell for converting solar radiation into electrical power [3], *J. Appl. Phys.*, 1954, **25**, 676–677, DOI: 10.1063/1.1721711.

36 X. Yin, Z. Song, Z. Li and W. Tang, Toward ideal hole transport materials: a review on recent progress in dopant-free hole transport materials for fabricating efficient and stable perovskite solar cells, *Energy Environ. Sci.*, 2020, **13**, 4057–4086, DOI: 10.1039/d0ee02337j.

37 W. Yan, Y. Li, Y. Li, S. Ye, Z. Liu, S. Wang, Z. Bian and C. Huang, High-performance hybrid perovskite solar cells with open circuit voltage dependence on hole-transporting materials, *Nano Energy*, 2015, **16**, 428–437, DOI: 10.1016/j.nanoen.2015.07.024.

38 W. Ke, P. Priyanka, S. Vegiraju, C. C. Stoumpos, I. Spanopoulos, C. M. M. Soe, T. J. Marks, M. C. Chen and M. G. Kanatzidis, Dopant-Free Tetrakis-Triphenylamine Hole Transporting Material for Efficient Tin-Based Perovskite Solar Cells, *J. Am. Chem. Soc.*, 2018, **140**, 388–393, DOI: 10.1021/jacs.7b10898.

39 C. Xu, Z. Liu and E. C. Lee, High-performance metal oxide-free inverted perovskite solar cells using poly(bis(4-phenyl)(2,4,6-trimethylphenyl)amine) as the hole transport layer, *J. Mater. Chem. C*, 2018, **6**, 6975–6981, DOI: 10.1039/C8TC02241K.

40 M. Ikram, M. Imran, J. M. Nunzi, Islah-U-Din and S. Ali, Replacement of P3HT and PCBM with metal oxides nanoparticles in inverted hybrid organic solar cells, *Synth. Met.*, 2015, **210**, 268–272, DOI: 10.1016/j.synthmet.2015.10.005.

41 S. Akin, Y. Altintas, E. Mutlugun and S. Sonmezoglu, Cesium–lead based inorganic perovskite quantum-dots as interfacial layer for highly stable perovskite solar cells with exceeding 21% efficiency, *Nano Energy*, 2019, **60**, 557–566, DOI: 10.1016/j.nanoen.2019.03.091.

42 L. Hu, W. Wang, H. Liu, J. Peng, H. Cao, G. Shao, Z. Xia, W. Ma and J. Tang, PbS colloidal quantum dots as an effective hole transporter for planar heterojunction perovskite solar cells, *J. Mater. Chem. A*, 2015, **3**, 516–518, DOI: 10.1039/c4ta04272g.

43 M. I. Hossain, F. H. Alharbi and N. Tabet, Copper oxide as inorganic hole transport material for lead halide perovskite based solar cells, *Sol. Energy*, 2015, **120**, 370–380, DOI: 10.1016/j.solener.2015.07.040.

44 V. E. Madhavan, I. Zimmermann, C. Roldán-Carmona, G. Grancini, M. Buffiere, A. Belaidi and M. K. Nazeeruddin, Copper Thiocyanate Inorganic Hole-Transporting Material for High-Efficiency Perovskite Solar Cells, *ACS Energy Lett.*, 2016, **1**, 1112–1117, DOI: 10.1021/acsenergylett.6b00501.

45 G. A. Sepalage, S. Meyer, A. Pascoe, A. D. Scully, F. Huang, U. Bach, Y. B. Cheng and L. Spiccia, Copper(I) Iodide as Hole-Conductor in Planar Perovskite Solar Cells: Probing the Origin of J-V Hysteresis, *Adv. Funct. Mater.*, 2015, **25**, 5650–5661, DOI: 10.1002/adfm.201502541.

46 K. C. Wang, J. Y. Jeng, P. S. Shen, Y. C. Chang, E. W. G. Diau, C. H. Tsai, T. Y. Chao, H. C. Hsu, P. Y. Lin, P. Chen, T. F. Guo and T. C. Wen, P-type mesoscopic nickel oxide/organometallic perovskite heterojunction solar cells, *Sci. Rep.*, 2014, **4**, 4756, DOI: 10.1038/srep04756.

47 B. S. Kim, T. M. Kim, M. S. Choi, H. S. Shim and J. J. Kim, Fully vacuum-processed perovskite solar cells with high open circuit voltage using MoO3/NPB as hole extraction

layers, *Org. Electron.*, 2015, **17**, 102–106, DOI: 10.1016/j.orgel.2014.12.002.

48 K. Aitola, K. Sveinbjörnsson, J. P. Correa-Baena, A. Kaskela, A. Abate, Y. Tian, E. M. J. Johansson, M. Grätzel, E. I. Kauppinen, A. Hagfeldt and G. Boschloo, Carbon nanotube-based hybrid hole-transporting material and selective contact for high efficiency perovskite solar cells, *Energy Environ. Sci.*, 2016, **9**, 461–466, DOI: 10.1039/c5ee03394b.

49 I. J. Park, M. A. Park, D. H. Kim, G. Do Park, B. J. Kim, H. J. Son, M. J. Ko, D. K. Lee, T. Park, H. Shin, N. G. Park, H. S. Jung and J. Y. Kim, New Hybrid Hole Extraction Layer of Perovskite Solar Cells with a Planar p-i-n Geometry, *J. Phys. Chem. C*, 2015, **119**, 27285–27290, DOI: 10.1021/acs.jpcc.5b09322.

50 J. Kim, K. S. Kim and C. W. Myung, Efficient electron extraction of SnO2 electron transport layer for lead halide perovskite solar cell, *npj Comput. Mater.*, 2020, **6**, 1–8, DOI: 10.1038/s41524-020-00370-y.

51 N. Wang, K. Zhao, T. Ding, W. Liu, A. S. Ahmed, Z. Wang, M. Tian, X. W. Sun and Q. Zhang, Improving Interfacial Charge Recombination in Planar Heterojunction Perovskite Photovoltaics with Small Molecule as Electron Transport Layer, *Adv. Energy Mater.*, 2017, **7**, 17000522, DOI: 10.1002/aenm.201700522.

52 M. Thambidurai, F. Shini, J. Y. Kim, C. Lee and C. Dang, Solution-processed Ga-TiO2 electron transport layer for efficient inverted organic solar cells, *Mater. Lett.*, 2020, **274**, 128003, DOI: 10.1016/j.matlet.2020.128003.

53 P. Zhang, J. Wu, T. Zhang, Y. Wang, D. Liu, H. Chen, L. Ji, C. Liu, W. Ahmad, Z. D. Chen and S. Li, Perovskite Solar Cells with ZnO Electron-Transporting Materials, *Adv. Mater.*, 2018, **30**, 1703737, DOI: 10.1002/adma.201703737.

54 H. Zhang, L. Xue, J. Han, Y. Q. Fu, Y. Shen, Z. Zhang, Y. Li and M. Wang, New generation perovskite solar cells with solution-processed amino-substituted perylene diimide derivative as electron-transport layer, *J. Mater. Chem. A*, 2016, **4**, 8724–8733, DOI: 10.1039/c6ta03119f.

55 F. Xia, Q. Wu, P. Zhou, Y. Li, X. Chen, Q. Liu, J. Zhu, S. Dai, Y. Lu and S. Yang, Efficiency Enhancement of Inverted Structure Perovskite Solar Cells via Oleamide Doping of PCBM Electron Transport Layer, *ACS Appl. Mater. Interfaces*, 2015, **7**, 13659–13665, DOI: 10.1021/acsami.5b03525.

56 C. L. Tsai, Y. C. Lu, S. E. Chiang, C. M. Yu, H. M. Cheng, C. L. Hsu, K. Y. Chiu and S. H. Chang, Bright and fast-response perovskite light-emitting diodes with an ICBA:modified-C60 nanocomposite electrical confinement layer, *Nanoscale*, 2020, **12**, 4061–4068, DOI: 10.1039/c9nr10246a.

57 A. Raj, M. Kumar, A. Kumar, A. Laref, K. Singh, S. Sharma and A. Anshul, Effect of doping engineering in TiO2 electron transport layer on photovoltaic performance of perovskite solar cells, *Mater. Lett.*, 2022, **313**, 131692, DOI: 10.1016/j.matlet.2022.131692.

58 K. Deng, Q. Chen and L. Li, Modification Engineering in SnO2 Electron Transport Layer toward Perovskite Solar Cells: Efficiency and Stability, *Adv. Funct. Mater.*, 2020, **30**, 2004209, DOI: 10.1002/adfm.202004209.

59 K. Mahmood, A. Khalid and M. T. Mehran, Nanostructured ZnO electron transporting materials for hysteresis-free perovskite solar cells, *Sol. Energy*, 2018, **173**, 496–503, DOI: 10.1016/j.solener.2018.08.004.

60 J. Fan, B. Jia and M. Gu, Perovskite-based low-cost and high-efficiency hybrid halide solar cells, *Photonics Res.*, 2014, **2**, 111, DOI: 10.1364/prj.2.000111.

61 D. H. Fabini, T. Hogan, H. A. Evans, C. C. Stoumpos, M. G. Kanatzidis and R. Seshadri, Dielectric and Thermodynamic Signatures of Low-Temperature Glassy Dynamics in the Hybrid Perovskites CH3NH3PbI3 and HC(NH2)2PbI3, *J. Phys. Chem. Lett.*, 2016, **7**, 376–381, DOI: 10.1021/acs.jpclett.5b02821.

62 J. P. Correa-Baena, M. Saliba, T. Buonassisi, M. Grätzel, A. Abate, W. Tress and A. Hagfeldt, Promises and challenges of perovskite solar cells, *Science*, 2017, **358**, 739–744, DOI: 10.1126/science.aam6323.

63 X. Li, D. Bi, C. Yi, J. D. Décoppet, J. Luo, S. M. Zakeeruddin, A. Hagfeldt and M. Grätzel, A vacuum flash-assisted solution process for high-efficiency large-area perovskite solar cells, *Science*, 2016, **353**, 58–62, DOI: 10.1126/science.aaf8060.

64 A. Sharenko and M. F. Toney, Relationships between Lead Halide Perovskite Thin-Film Fabrication, Morphology, and Performance in Solar Cells, *J. Am. Chem. Soc.*, 2016, **138**, 463–470, DOI: 10.1021/jacs.5b10723.

65 X. Guo, J. Li, B. Wang, P. Zeng, F. Li, Q. Yang, Y. Chen and M. Liu, Improving and Stabilizing Perovskite Solar Cells with Incorporation of Graphene in the Spiro-OMeTAD Layer: Suppressed Li Ions Migration and Improved Charge Extraction, *ACS Appl. Energy Mater.*, 2020, **3**, 970–976, DOI: 10.1021/acsaem.9b02037.

66 Q. Q. Chu, B. Ding, J. Peng, H. Shen, X. Li, Y. Liu, C. X. Li, C. J. Li, G. J. Yang, T. P. White and K. R. Catchpole, Highly stable carbon-based perovskite solar cell with a record efficiency of over 18% via hole transport engineering, *J. Mater. Sci. Technol.*, 2019, **35**, 987–993, DOI: 10.1016/j.jmst.2018.12.025.

67 E. Muchuweni, T. S. Sathiaraj and H. Nyakotyo, Low temperature synthesis of radio frequency magnetron sputtered gallium and aluminium co-doped zinc oxide thin films for transparent electrode fabrication, *Appl. Surf. Sci.*, 2016, **390**, 570–577, DOI: 10.1016/j.apsusc.2016.08.081.

68 E. Muchuweni, T. S. Sathiaraj and H. Nyakotyo, Effect of gallium doping on the structural, optical and electrical properties of zinc oxide thin films prepared by spray pyrolysis, *Ceram. Int.*, 2016, **42**, 10066–10070, DOI: 10.1016/j.ceramint.2016.03.110.

69 D. G. Papageorgiou, I. A. Kinloch and R. J. Young, Mechanical properties of graphene and graphene-based nanocomposites, *Prog. Mater. Sci.*, 2017, **90**, 75–127, DOI: 10.1016/j.pmatsci.2017.07.004.

70 Q. G. Du, G. Shen and S. John, Light-trapping in perovskite solar cells, *AIP Adv.*, 2016, **6**, DOI: 10.1063/1.4953336.

71 S. Foster and S. John, Light-trapping design for thin-film silicon-perovskite tandem solar cells, *J. Appl. Phys.*, 2016, **120**, DOI: 10.1063/1.4962458.
72 J. Zhuang, P. Mao, Y. Luan, N. Chen, X. Cao, G. Niu, F. Jia, F. Wang, S. Cao and J. Wang, Rubidium Fluoride Modified SnO2 for Planar n-i-p Perovskite Solar Cells, *Adv. Funct. Mater.*, 2021, **31**, 2010385, DOI: 10.1002/adfm.202010385.
73 C. Wang, J. Wu, S. Wang, X. Liu, X. Wang, Z. Yan, L. Chen, X. Liu, G. Li, W. Sun and Z. Lan, Alkali Metal Fluoride-Modified Tin Oxide for n-i-p Planar Perovskite Solar Cells, *ACS Appl. Mater. Interfaces*, 2021, **13**, 50083–50092, DOI: 10.1021/acsami.1c16519.
74 R. Wang, M. Mujahid, Y. Duan, Z. K. Wang, J. Xue and Y. Yang, A Review of Perovskites Solar Cell Stability, *Adv. Funct. Mater.*, 2019, **29**, 1808843, DOI: 10.1002/adfm.201808843.
75 M. Wang, H. Wang, W. Li, X. Hu, K. Sun and Z. Zang, Defect passivation using ultrathin PTAA layers for efficient and stable perovskite solar cells with a high fill factor and eliminated hysteresis, *J. Mater. Chem. A*, 2019, **7**, 26421–26428, DOI: 10.1039/c9ta08314f.
76 L. Xu, Y. Li, C. Zhang, Y. Liu, C. Zheng, W. Z. Lv, M. Li, Y. Chen, W. Huang and R. Chen, Improving the efficiency and stability of inverted perovskite solar cells by CuSCN-doped PEDOT:PSS, *Sol. Energy Mater. Sol. Cells*, 2020, **206**, 110316, DOI: 10.1016/j.solmat.2019.110316.
77 W. Li, N. Cheng, Y. Cao, Z. Zhao, Z. Xiao, W. Zi and Z. Sun, Boost the performance of inverted perovskite solar cells with PEDOT:PSS/Graphene quantum dots composite hole transporting layer, *Org. Electron.*, 2019, **78**, 105575, DOI: 10.1016/j.orgel.2019.105575.
78 X. Zheng, Y. Hou, C. Bao, J. Yin, F. Yuan, Z. Huang, K. Song, J. Liu, J. Troughton, N. Gasparini, C. Zhou, Y. Lin, D. J. Xue, B. Chen, A. K. Johnston, N. Wei, M. N. Hedhili, M. Wei, A. Y. Alsalloum, P. Maity, B. Turedi, C. Yang, D. Baran, T. D. Anthopoulos, Y. Han, Z. H. Lu, O. F. Mohammed, F. Gao, E. H. Sargent and O. M. Bakr, Managing grains and interfaces via ligand anchoring enables 22.3%-efficiency inverted perovskite solar cells, *Nat. Energy*, 2020, **5**, 131–140, DOI: 10.1038/s41560-019-0538-4.
79 D. Ramirez, K. Schutt, J. F. Montoya, S. Mesa, J. Lim, H. J. Snaith and F. Jaramillo, Meso-Superstructured Perovskite Solar Cells: Revealing the Role of the Mesoporous Layer, *J. Phys. Chem. C*, 2018, **122**, 21239–21247, DOI: 10.1021/acs.jpcc.8b07124.
80 X. Li, J. Yang, Q. Jiang, H. Lai, S. Li, Y. Tan, Y. Chen and S. Li, Perovskite solar cells employing an eco-friendly and low-cost inorganic hole transport layer for enhanced photovoltaic performance and operational stability, *J. Mater. Chem. A*, 2019, **7**, 7065–7073, DOI: 10.1039/c9ta01499c.
81 E. Widianto, Shobih, E. S. Rosa, K. Triyana, N. M. Nursam and I. Santoso, Graphene oxide as an effective hole transport material for low-cost carbon-based mesoscopic perovskite solar cells, *Adv. Nat. Sci.: Nanosci. Nanotechnol.*, 2021, **12**, 35001, DOI: 10.1088/2043-6262/ac204a.
82 G. Li, K. Deng, Y. Dou, Y. Liao, D. Wang, J. Wu and Z. Lan, Self-assembled NiO microspheres for efficient inverted mesoscopic perovskite solar cells, *Sol. Energy*, 2019, **193**, 111–117, DOI: 10.1016/j.solener.2019.09.064.
83 X. Yin, J. Zhai, L. Song, P. Du, N. Li, Y. Yang, J. Xiong and F. Ko, Novel NiO Nanoforest Architecture for Efficient Inverted Mesoporous Perovskite Solar Cells, *ACS Appl. Mater. Interfaces*, 2019, **11**, 44308–44314, DOI: 10.1021/acsami.9b15820.
84 L. Lin, P. Li, L. Jiang, Z. Kang, Q. Yan, H. Xiong, S. Lien, P. Zhang and Y. Qiu, Boosting efficiency up to 25% for HTL-free carbon-based perovskite solar cells by gradient doping using SCAPS simulation, *Sol. Energy*, 2021, **215**, 328–334, DOI: 10.1016/j.solener.2020.12.059.
85 A. K. Al-Mousoi and M. K. A. Mohammed, Engineered surface properties of MAPI using different antisolvents for hole transport layer-free perovskite solar cell (HTL-free PSC), *J. Sol-Gel Sci. Technol.*, 2020, **96**, 659–668, DOI: 10.1007/s10971-020-05380-2.
86 H. Pourfarzad, M. Saremi and R. Badrnezhad, Study of performance and stability of hole transport layer-free perovskite solar cells with modified electron transport layer, *J. Mater. Sci.: Mater. Electron.*, 2021, **32**, 17602–17611, DOI: 10.1007/s10854-021-06293-8.
87 F. Sadegh, E. Akman, D. Prochowicz, M. M. Tavakoli, P. Yadav and S. Akin, Facile NaF Treatment Achieves 20% Efficient ETL-Free Perovskite Solar Cells, *ACS Appl. Mater. Interfaces*, 2022, **14**, 38641, DOI: 10.1021/acsami.2c06110.
88 L. Huang, J. Huang, R. Peng and Z. Ge, Efficient Electron Transport Layer-Free Perovskite Solar Cells Enabled by Discontinuous Polar Molecular Films: A Story of New Materials and Old Ideas?, *ACS Sustain. Chem. Eng.*, 2021, **9**, 936–943, DOI: 10.1021/acssuschemeng.0c08217.
89 J. Wang, S. Fu, L. Huang, Y. Lu, X. Liu, J. Zhang, Z. Hu and Y. Zhu, Heterojunction Engineering and Ideal Factor Optimization Toward Efficient MINP Perovskite Solar Cells, *Adv. Energy Mater.*, 2021, **11**, 2102724, DOI: 10.1002/aenm.202102724.
90 H. Duan, X. Li, Y. Gou, H. Wang, L. Fan, Y. Chen, J. Yang, L. Yang and F. Wang, A two-fold interfacial electric-field strategy: boosting the performance of electron transport layer-free perovskite solar cells with low-cost and versatile inorganic acid treatment, *J. Mater. Chem. C*, 2021, **9**, 12920–12927, DOI: 10.1039/d1tc03246a.
91 T. A. Chowdhury, M. A. Bin Zafar, M. Sajjad-Ul Islam, M. Shahinuzzaman, M. A. Islam and M. U. Khandaker, Stability of perovskite solar cells: issues and prospects, *RSC Adv.*, 2023, **13**, 1787–1810, DOI: 10.1039/d2ra05903g.
92 F. Wang, T. Zhang, Y. Wang, D. Liu, P. Zhang, H. Chen, L. Ji, L. Chen, Z. D. Chen, J. Wu, X. Liu, Y. Li and S. Li, Steering the crystallization of perovskites for high-performance solar cells in ambient air, *J. Mater. Chem. A*, 2019, **7**, 12166–12175, DOI: 10.1039/c9ta02566a.
93 J. M. Frost, K. T. Butler, F. Brivio, C. H. Hendon, M. Van Schilfgaarde and A. Walsh, Atomistic origins of high-performance in hybrid halide perovskite solar cells, *Nano Lett.*, 2014, **14**, 2584–2590, DOI: 10.1021/nl500390f.

94 H. D. Pham, T. C. J. Yang, S. M. Jain, G. J. Wilson and P. Sonar, Development of Dopant-Free Organic Hole Transporting Materials for Perovskite Solar Cells, *Adv. Energy Mater.*, 2020, **10**, 1903326, DOI: 10.1002/aenm.201903326.

95 E. J. Juarez-Perez, L. K. Ono, M. Maeda, Y. Jiang, Z. Hawash and Y. Qi, Photodecomposition and thermal decomposition in methylammonium halide lead perovskites and inferred design principles to increase photovoltaic device stability, *J. Mater. Chem. A*, 2018, **6**, 9604–9612, DOI: 10.1039/c8ta03501f.

96 B. Conings, J. Drijkoningen, N. Gauquelin, A. Babayigit, J. D'Haen, L. D'Olieslaeger, A. Ethirajan, J. Verbeeck, J. Manca, E. Mosconi, F. De Angelis and H. G. Boyen, Intrinsic Thermal Instability of Methylammonium Lead Trihalide Perovskite, *Adv. Energy Mater.*, 2015, **5**, 1500477, DOI: 10.1002/aenm.201500477.

97 E. J. Juarez-Perez, Z. Hawash, S. R. Raga, L. K. Ono and Y. Qi, Thermal degradation of $CH_3NH_3PbI_3$ perovskite into NH_3 and CH_3I gases observed by coupled thermogravimetry–mass spectrometry analysis, *Energy Environ. Sci.*, 2016, **9**(11), 3406–3410.

98 A. Latini, G. Gigli and A. Ciccioli, A study on the nature of the thermal decomposition of methylammonium lead iodide perovskite, CH3NH3PbI3: an attempt to rationalise contradictory experimental results, *Sustainable Energy Fuels*, 2017, **1**, 1351–1357, DOI: 10.1039/c7se00114b.

99 Z. Wang, D. P. McMeekin, N. Sakai, S. van Reenen, K. Wojciechowski, J. B. Patel, M. B. Johnston and H. J. Snaith, Efficient and Air-Stable Mixed-Cation Lead Mixed-Halide Perovskite Solar Cells with n-Doped Organic Electron Extraction Layers, *Adv. Mater.*, 2017, **29**, 1604186, DOI: 10.1002/adma.201604186.

100 A. J. Pearson, G. E. Eperon, P. E. Hopkinson, S. N. Habisreutinger, J. T. W. Wang, H. J. Snaith and N. C. Greenham, Oxygen Degradation in Mesoporous Al2O3/CH3NH3PbI3-xClx Perovskite Solar Cells: Kinetics and Mechanisms, *Adv. Energy Mater.*, 2016, **6**, 1600014, DOI: 10.1002/aenm.201600014.

101 N. Aristidou, C. Eames, I. Sanchez-Molina, X. Bu, J. Kosco, M. Saiful Islam and S. A. Haque, Fast oxygen diffusion and iodide defects mediate oxygen-induced degradation of perovskite solar cells, *Nat. Commun.*, 2017, **8**, 15218, DOI: 10.1038/ncomms15218.

102 Q. Fu, X. Tang, B. Huang, T. Hu, L. Tan, L. Chen and Y. Chen, Recent Progress on the Long-Term Stability of Perovskite Solar Cells, *Adv. Sci.*, 2018, **5**, 1700387, DOI: 10.1002/advs.201700387.

103 J. S. Shaikh, N. S. Shaikh, A. D. Sheikh, S. S. Mali, A. J. Kale, P. Kanjanaboos, C. K. Hong, J. H. Kim and P. S. Patil, Perovskite solar cells: in pursuit of efficiency and stability, *Mater. Des.*, 2017, **136**, 54–80, DOI: 10.1016/j.matdes.2017.09.037.

104 A. K. Jena, A. Kulkarni and T. Miyasaka, Halide Perovskite Photovoltaics: Background, Status, and Future Prospects, *Chem. Rev.*, 2019, **119**, 3036–3103, DOI: 10.1021/acs.chemrev.8b00539.

105 L. Dimesso, C. Wittich, T. Mayer and W. Jaegermann, Phase-change behavior of hot-pressed methylammonium lead bromide hybrid perovskites, *J. Mater. Sci.*, 2019, **54**, 2001–2015, DOI: 10.1007/s10853-018-3009-6.

106 W. Chi and S. K. Banerjee, Achieving Resistance against Moisture and Oxygen for Perovskite Solar Cells with High Efficiency and Stability, *Chem. Mater.*, 2021, **33**, 4269–4303, DOI: 10.1021/acs.chemmater.1c00773.

107 Y. Takahashi, H. Hasegawa, Y. Takahashi and T. Inabe, Hall mobility in tin iodide perovskite CH3NH3SnI 3: evidence for a doped semiconductor, *J. Solid State Chem.*, 2013, **205**, 39–43, DOI: 10.1016/j.jssc.2013.07.008.

108 M. B. Johnston and L. M. Herz, Hybrid Perovskites for Photovoltaics: Charge-Carrier Recombination, Diffusion, and Radiative Efficiencies, *Acc. Chem. Res.*, 2016, **49**, 146–154, DOI: 10.1021/acs.accounts.5b00411.

109 S. Gupta, D. Cahen and G. Hodes, How SnF2 Impacts the Material Properties of Lead-Free Tin Perovskites, *J. Phys. Chem. C*, 2018, **122**, 13926–13936, DOI: 10.1021/acs.jpcc.8b01045.

110 L. Lanzetta, T. Webb, N. Zibouche, X. Liang, D. Ding, G. Min, R. J. E. Westbrook, B. Gaggio, T. J. Macdonald, M. S. Islam and S. A. Haque, Degradation mechanism of hybrid tin-based perovskite solar cells and the critical role of tin (IV) iodide, *Nat. Commun.*, 2021, **12**, 1–11, DOI: 10.1038/s41467-021-22864-z.

111 S. K. Podapangi, F. Jafarzadeh, S. Mattiello, T. B. Korukonda, A. Singh, L. Beverina and T. M. Brown, Green solvents, materials, and lead-free semiconductors for sustainable fabrication of perovskite solar cells, *RSC Adv.*, 2023, **13**, 18165–18206, DOI: 10.1039/d3ra01692g.

112 S. Macpherson, T. A. S. Doherty, A. J. Winchester, S. Kosar, D. N. Johnstone, Y. H. Chiang, K. Galkowski, M. Anaya, K. Frohna, A. N. Iqbal, S. Nagane, B. Roose, Z. Andaji-Garmaroudi, K. W. P. Orr, J. E. Parker, P. A. Midgley, K. M. Dani and S. D. Stranks, Local nanoscale phase impurities are degradation sites in halide perovskites, *Nature*, 2022, **607**, 294–300, DOI: 10.1038/s41586-022-04872-1.

113 W. Zhang, X. Li, S. Fu, X. Zhao, X. Feng and J. Fang, Lead-lean and MA-free perovskite solar cells with an efficiency over 20%, *Joule*, 2021, **5**, 2904–2914, DOI: 10.1016/j.joule.2021.09.008.

114 Q. Wang, B. Chen, Y. Liu, Y. Deng, Y. Bai, Q. Dong and J. Huang, Scaling behavior of moisture-induced grain degradation in polycrystalline hybrid perovskite thin films, *Energy Environ. Sci.*, 2017, **10**, 516–522, DOI: 10.1039/c6ee02941h.

115 H. Mehdizadeh-Rad, F. Mehdizadeh-Rad, F. Zhu and J. Singh, Heat mitigation in perovskite solar cells: the role of grain boundaries, *Sol. Energy Mater. Sol. Cells*, 2021, **220**, 110837, DOI: 10.1016/j.solmat.2020.110837.

116 D. Knig, K. Casalenuovo, Y. Takeda, G. Conibeer, J. F. Guillemoles, R. Patterson, L. M. Huang and M. A. Green, Hot carrier solar cells: principles, materials and design, *Phys. E*, 2010, 2862–2866, DOI: 10.1016/j.physe.2009.12.032.

117 T. S. Sherkar, C. Momblona, L. Gil-Escrig, J. Ávila, M. Sessolo, H. J. Bolink and L. J. A. Koster, Recombination in Perovskite Solar Cells: Significance of Grain Boundaries, Interface Traps, and Defect Ions, *ACS Energy Lett.*, 2017, **2**, 1214–1222, DOI: **10.1021/acsenergylett.7b00236**.

118 E. Yandri and N. Hagino, Joule heating estimation of photovoltaic module through cells temperature measurement, *Int. J. Power Electron. Drive Syst.*, 2022, **13**, 1119–1128, DOI: **10.11591/ijpeds.v13.i2.pp1119-1128**.

119 A. Shang, Y. An, D. Ma and X. Li, Optoelectronic insights into the photovoltaic losses from photocurrent, voltage, and energy perspectives, *AIP Adv.*, 2017, **7**, DOI: **10.1063/1.4990288**.

120 S. Zandi, M. J. Seresht, A. Khan and N. E. Gorji, Simulation of heat loss in Cu2ZnSn4SxSe4−x thin film solar cells: a coupled optical-electrical-thermal modeling, *Renewable Energy*, 2022, **181**, 320–328, DOI: **10.1016/j.renene.2021.09.035**.

121 Z. Wu, M. Zhang, Y. Liu, Y. Dou, Y. Kong, L. Gao, W. Han, G. Liang, X. L. Zhang, F. Huang, Y. B. Cheng and J. Zhong, Groups-dependent phosphines as the organic redox for point defects elimination in hybrid perovskite solar cells, *J. Energy Chem.*, 2020, **54**, 23–29, DOI: **10.1016/j.jechem.2020.05.047**.

122 Y. Wang, T. Mahmoudi, W. Y. Rho and Y. B. Hahn, Fully-ambient-air and antisolvent-free-processed stable perovskite solar cells with perovskite-based composites and interface engineering, *Nano Energy*, 2019, **64**, 103964, DOI: **10.1016/j.nanoen.2019.103964**.

123 B. Ghosh, D. J. J. Tay, M. B. J. Roeffaers and N. Mathews, Lead-free metal halide (halogenidometallate) semiconductors for optoelectronic applications, *Appl. Phys. Rev.*, 2023, **10**, DOI: **10.1063/5.0150873**.

124 M. Ren, X. Qian, Y. Chen, T. Wang and Y. Zhao, Potential lead toxicity and leakage issues on lead halide perovskite photovoltaics, *J. Hazard. Mater.*, 2022, **426**, 127848, DOI: **10.1016/j.jhazmat.2021.127848**.

125 U. Zulfiqar, M. Farooq, S. Hussain, M. Maqsood, M. Hussain, M. Ishfaq, M. Ahmad and M. Z. Anjum, Lead toxicity in plants: impacts and remediation, *J. Environ. Manage.*, 2019, **250**, 109557, DOI: **10.1016/j.jenvman.2019.109557**.

126 X. Jin, Y. Yang, T. Zhao, X. Wu, B. Liu, M. Han, W. Chen, T. Chen, J. S. Hu and Y. Jiang, Mitigating Potential Lead Leakage Risk of Perovskite Solar Cells by Device Architecture Engineering from Exterior to Interior, *ACS Energy Lett.*, 2022, **7**, 3618–3636, DOI: **10.1021/acsenergylett.2c01602**.

127 P. Wu, S. Wang, X. Li and F. Zhang, Beyond efficiency fever: preventing lead leakage for perovskite solar cells, *Matter*, 2022, **5**, 1137–1161, DOI: **10.1016/j.matt.2022.02.012**.

128 Y. Gao, Y. Hu, C. Yao and S. Zhang, Recent Advances in Lead-Safe Perovskite Solar Cells, *Adv. Funct. Mater.*, 2022, **32**, 2208225, DOI: **10.1002/adfm.202208225**.

129 J. Chen, S. Li, T. Ma, D. Wu, Y. Zhao, C. Wang, D. Zhao and X. Li, Managing Lead Leakage in Efficient Perovskite Solar Cells with Phosphate Interlayers, *Adv. Mater. Interfaces*, 2022, **9**, 2200570, DOI: **10.1002/admi.202200570**.

130 B. Niu, H. Wu, J. Yin, B. Wang, G. Wu, X. Kong, B. Yan, J. Yao, C. Z. Li and H. Chen, Mitigating the Lead Leakage of High-Performance Perovskite Solar Cells via in Situ Polymerized Networks, *ACS Energy Lett.*, 2021, **6**, 3443–3449, DOI: **10.1021/acsenergylett.1c01487**.

131 X. Meng, X. Hu, Y. Zhang, Z. Huang, Z. Xing, C. Gong, L. Rao, H. Wang, F. Wang, T. Hu, L. Tan, Y. Song and Y. Chen, A Biomimetic Self-Shield Interface for Flexible Perovskite Solar Cells with Negligible Lead Leakage, *Adv. Funct. Mater.*, 2021, **31**(52), 2106460, DOI: **10.1002/adfm.202106460**.

132 Z. He, Y. Hu, G. Sun, W. Song, X. Wang, S. Zhang, J. Wang, M. Wang, T. Sun and Y. Tang, Simultaneous Chemical Crosslinking of SnO2 and Perovskite for High-Performance Planar Perovskite Solar Cells with Minimized Lead Leakage, *Sol. RRL*, 2022, **6**, 2200567, DOI: **10.1002/solr.202200567**.

133 A. Agresti, S. Pescetelli, L. Cinà, D. Konios, G. Kakavelakis, E. Kymakis and A. Di Carlo, Efficiency and Stability Enhancement in Perovskite Solar Cells by Inserting Lithium-Neutralized Graphene Oxide as Electron Transporting Layer, *Adv. Funct. Mater.*, 2016, **26**, 2686–2694, DOI: **10.1002/adfm.201504949**.

134 S. Guarnera, A. Abate, W. Zhang, J. M. Foster, G. Richardson, A. Petrozza and H. J. Snaith, Improving the long-term stability of perovskite solar cells with a porous Al2O3 buffer layer, *J. Phys. Chem. Lett.*, 2015, **6**, 432–437, DOI: **10.1021/jz502703p**.

135 T. Leijtens, G. E. Eperon, S. Pathak, A. Abate, M. M. Lee and H. J. Snaith, Overcoming ultraviolet light instability of sensitized TiO2 with meso-superstructured organometal tri-halide perovskite solar cells, *Nat. Commun.*, 2013, **4**(1), 2885, DOI: **10.1038/ncomms3885**.

136 Y. Duan, X. Wang, Y. H. Duan, Y. Q. Yang, P. Chen, D. Yang, F. B. Sun, K. W. Xue, N. Hu and J. W. Hou, High-performance barrier using a dual-layer inorganic/organic hybrid thin-film encapsulation for organic light-emitting diodes, *Org. Electron.*, 2014, **15**, 1936–1941, DOI: **10.1016/j.orgel.2014.05.001**.

137 F. Liu, Q. Dong, M. K. Wong, A. B. Djurišić, A. Ng, Z. Ren, Q. Shen, C. Surya, W. K. Chan, J. Wang, A. M. C. Ng, C. Liao, H. Li, K. Shih, C. Wei, H. Su and J. Dai, Is Excess PbI2 Beneficial for Perovskite Solar Cell Performance?, *Adv. Energy Mater.*, 2016, **6**, 1502206, DOI: **10.1002/aenm.201502206**.

138 B. Li, Y. Li, C. Zheng, D. Gao and W. Huang, Advancements in the stability of perovskite solar cells: degradation mechanisms and improvement approaches, *RSC Adv.*, 2016, **6**, 38079–38091, DOI: **10.1039/c5ra27424a**.

139 F. C. Krebs, S. A. Gevorgyan and J. Alstrup, A roll-to-roll process to flexible polymer solar cells: model studies, manufacture and operational stability studies, *J. Mater. Chem.*, 2009, **19**, 5442–5451, DOI: **10.1039/b823001c**.

140 A. S. da Silva Sobrinho, M. Latrèche, G. Czeremuszkin, J. E. Klemberg-Sapieha and M. R. Wertheimer,

Transparent barrier coatings on polyethylene terephthalate by single- and dual-frequency plasma-enhanced chemical vapor deposition, *J. Vac. Sci. Technol., A*, 1998, **16**, 3190–3198, DOI: 10.1116/1.581519.

141 N. Kim, W. J. Potscavage, A. Sundaramoothi, C. Henderson, B. Kippelen and S. Graham, A correlation study between barrier film performance and shelf lifetime of encapsulated organic solar cells, *Sol. Energy Mater. Sol. Cells*, 2012, **101**, 140–146, DOI: 10.1016/j.solmat.2012.02.002.

142 J. Ahmad, K. Bazaka, L. J. Anderson, R. D. White and M. V. Jacob, Materials and methods for encapsulation of OPV: a review, *Renewable Sustainable Energy Rev.*, 2013, **27**, 104–117, DOI: 10.1016/j.rser.2013.06.027.

143 I. Hwang, I. Jeong, J. Lee, M. J. Ko and K. Yong, Enhancing Stability of Perovskite Solar Cells to Moisture by the Facile Hydrophobic Passivation, *ACS Appl. Mater. Interfaces*, 2015, **7**, 17330–17336, DOI: 10.1021/acsami.5b04490.

144 C. Y. Chang, K. T. Lee, W. K. Huang, H. Y. Siao and Y. C. Chang, High-Performance, Air-Stable, Low-Temperature Processed Semitransparent Perovskite Solar Cells Enabled by Atomic Layer Deposition, *Chem. Mater.*, 2015, **27**, 5122–5130, DOI: 10.1021/acs.chemmater.5b01933.

145 J. Idígoras, F. J. Aparicio, L. Contreras-Bernal, S. Ramos-Terrón, M. Alcaire, J. R. Sánchez-Valencia, A. Borras, Á. Barranco and J. A. Anta, Enhancing Moisture and Water Resistance in Perovskite Solar Cells by Encapsulation with Ultrathin Plasma Polymers, *ACS Appl. Mater. Interfaces*, 2018, **10**, 11587–11594, DOI: 10.1021/acsami.7b17824.

146 J. H. Noh, S. H. Im, J. H. Heo, T. N. Mandal and S. Il Seok, Chemical management for colorful, efficient, and stable inorganic-organic hybrid nanostructured solar cells, *Nano Lett.*, 2013, **13**, 1764–1769, DOI: 10.1021/nl400349b.

147 J. H. Noh, S. H. Im, J. H. Heo, T. N. Mandal and S. Il Seok, Chemical management for colorful, efficient, and stable inorganic-organic hybrid nanostructured solar cells, *Nano Lett.*, 2013, **13**, 1764–1769, DOI: 10.1021/NL400349B.

148 R. Ruess, F. Benfer, F. Böcher, M. Stumpp and D. Schlettwein, Stabilization of Organic-Inorganic Perovskite Layers by Partial Substitution of Iodide by Bromide in Methylammonium Lead Iodide, *ChemPhysChem*, 2016, **17**, 1505–1511, DOI: 10.1002/cphc.201501168.

149 H. S. Kim, J. Y. Seo and N. G. Park, Material and Device Stability in Perovskite Solar Cells, *ChemSusChem*, 2016, **9**, 2528–2540, DOI: 10.1002/cssc.201600915.

150 E. Mosconi, J. M. Azpiroz and F. De Angelis, Ab Initio Molecular Dynamics Simulations of Methylammonium Lead Iodide Perovskite Degradation by Water, *Chem. Mater.*, 2015, **27**, 4885–4892, DOI: 10.1021/acs.chemmater.5b01991.

151 R. Ruess, F. Benfer, F. Böcher, M. Stumpp and D. Schlettwein, Stabilization of Organic-Inorganic Perovskite Layers by Partial Substitution of Iodide by Bromide in Methylammonium Lead Iodide, *ChemPhysChem*, 2016, **17**, 1505–1511, DOI: 10.1002/cphc.201501168.

152 I. C. Smith, E. T. Hoke, D. Solis-Ibarra, M. D. McGehee and H. I. Karunadasa, A Layered Hybrid Perovskite Solar-Cell Absorber with Enhanced Moisture Stability, *Angew. Chem., Int. Ed.*, 2014, **53**, 11232–11235, DOI: 10.1002/anie.201406466.

153 I. C. Smith, E. T. Hoke, D. Solis-Ibarra, M. D. McGehee and H. I. Karunadasa, A Layered Hybrid Perovskite Solar-Cell Absorber with Enhanced Moisture Stability, *Angew. Chem., Int. Ed.*, 2014, **53**, 11232–11235, DOI: 10.1002/anie.201406466.

154 N. K. Noel, S. D. Stranks, A. Abate, C. Wehrenfennig, S. Guarnera, A. A. Haghighirad, A. Sadhanala, G. E. Eperon, S. K. Pathak, M. B. Johnston, A. Petrozza, L. M. Herz and H. J. Snaith, Lead-free organic-inorganic tin halide perovskites for photovoltaic applications, *Energy Environ. Sci.*, 2014, **7**, 3061–3068, DOI: 10.1039/c4ee01076k.

155 N. Espinosa, L. Serrano-Luján, A. Urbina and F. C. Krebs, Solution and vapour deposited lead perovskite solar cells: ecotoxicity from a life cycle assessment perspective, *Sol. Energy Mater. Sol. Cells*, 2015, **137**, 303–310, DOI: 10.1016/j.solmat.2015.02.013.

156 F. Hao, C. C. Stoumpos, D. H. Cao, R. P. H. Chang and M. G. Kanatzidis, Lead-free solid-state organic-inorganic halide perovskite solar cells, *Nat. Photonics*, 2014, **8**, 489–494, DOI: 10.1038/nphoton.2014.82.

157 N. G. Park, Research Direction toward Scalable, Stable, and High Efficiency Perovskite Solar Cells, *Adv. Energy Mater.*, 2020, **10**, 1903106, DOI: 10.1002/aenm.201903106.

158 S. J. Adjogri and E. L. Meyer, A Review on Lead-Free Hybrid Halide Perovskites as Light Absorbers for Photovoltaic Applications Based on Their Structural, Optical, and Morphological Properties, *Molecules*, 2020, **25**(21), 5039, DOI: 10.3390/molecules25215039.

159 M. Konstantakou and T. Stergiopoulos, A critical review on tin halide perovskite solar cells, *J. Mater. Chem. A*, 2017, **5**, 11518–11549, DOI: 10.1039/c7ta00929a.

160 Z. Shi, J. Guo, Y. Chen, Q. Li, Y. Pan, H. Zhang, Y. Xia and W. Huang, Lead-Free Organic–Inorganic Hybrid Perovskites for Photovoltaic Applications: Recent Advances and Perspectives, *Adv. Mater.*, 2017, **29**(16), 1605005, DOI: 10.1002/adma.201605005.

161 M. Konstantakou and T. Stergiopoulos, A critical review on tin halide perovskite solar cells, *J. Mater. Chem. A*, 2017, **5**, 11518–11549, DOI: 10.1039/c7ta00929a.

162 H. Kim, Y. H. Lee, T. Lyu, J. H. Yoo, T. Park and J. H. Oh, Boosting the performance and stability of quasi-two-dimensional tin-based perovskite solar cells using the formamidinium thiocyanate additive, *J. Mater. Chem. A*, 2018, **6**, 18173–18182, DOI: 10.1039/c8ta05916k.

163 S. J. Lee, S. S. Shin, J. Im, T. K. Ahn, J. H. Noh, N. J. Jeon, S. Il Seok and J. Seo, Reducing Carrier Density in Formamidinium Tin Perovskites and Its Beneficial Effects on Stability and Efficiency of Perovskite Solar Cells, *ACS*

Energy Lett., 2018, **3**, 46–53, DOI: 10.1021/acsenergylett.7b00976.

164 J. Horn, M. Scholz, K. Oum, T. Lenzer and D. Schlettwein, Influence of phenylethylammonium iodide as additive in the formamidinium tin iodide perovskite on interfacial characteristics and charge carrier dynamics, *APL Mater.*, 2019, **7**, 31112, DOI: 10.1063/1.5083624.

165 S. Shao, J. Liu, G. Portale, H. H. Fang, G. R. Blake, G. H. ten Brink, L. J. A. Koster and M. A. Loi, Highly Reproducible Sn-Based Hybrid Perovskite Solar Cells with 9% Efficiency, *Adv. Energy Mater.*, 2018, **8**(4), 1702019, DOI: 10.1002/aenm.201702019.

166 X. L. Li, L. L. Gao, Q. Q. Chu, Y. Li, B. Ding and G. J. Yang, Green Solution-Processed Tin-Based Perovskite Films for Lead-Free Planar Photovoltaic Devices, *ACS Appl. Mater. Interfaces*, 2019, **11**, 3053–3060, DOI: 10.1021/acsami.8b19143.

167 X. Liu, K. Yan, D. Tan, X. Liang, H. Zhang and W. Huang, Solvent engineering improves efficiency of lead-free tin-based hybrid perovskite solar cells beyond 9%, *ACS Energy Lett.*, 2018, **3**, 2701–2707, DOI: 10.1021/acsenergylett.8b01588.

168 E. Jokar, C. H. Chien, A. Fathi, M. Rameez, Y. H. Chang and E. W. G. Diau, Slow surface passivation and crystal relaxation with additives to improve device performance and durability for tin-based perovskite solar cells, *Energy Environ. Sci.*, 2018, **11**, 2353–2362, DOI: 10.1039/c8ee00956b.

169 J. Cao, Q. Tai, P. You, G. Tang, T. Wang, N. Wang and F. Yan, Enhanced performance of tin-based perovskite solar cells induced by an ammonium hypophosphite additive, *J. Mater. Chem. A*, 2019, **7**, 26580–26585, DOI: 10.1039/c9ta08679j.

170 S. Vegiraju, W. Ke, P. Priyanka, J. S. Ni, Y. C. Wu, I. Spanopoulos, S. L. Yau, T. J. Marks, M. C. Chen and M. G. Kanatzidis, Benzodithiophene Hole-Transporting Materials for Efficient Tin-Based Perovskite Solar Cells, *Adv. Funct. Mater.*, 2019, **29**, 1905393, DOI: 10.1002/adfm.201905393.

171 X. Meng, J. Lin, X. Liu, X. He, Y. Wang, T. Noda, T. Wu, X. Yang and L. Han, Highly Stable and Efficient FASnI3-Based Perovskite Solar Cells by Introducing Hydrogen Bonding, *Adv. Mater.*, 2019, **31**, 1903721, DOI: 10.1002/adma.201903721.

172 J. Li, P. Hu, Y. Chen, Y. Li, M. Wei and M. Wei, Enhanced Performance of Sn-Based Perovskite Solar Cells by Two-Dimensional Perovskite Doping, *ACS Sustain. Chem. Eng.*, 2020, **8**, 8624–8628, DOI: 10.1021/acssuschemeng.0c01216.

173 T. Wu, X. Liu, X. He, Y. Wang, X. Meng, T. Noda, X. Yang and L. Han, Efficient and stable tin-based perovskite solar cells by introducing $π$-conjugated Lewis base, *Sci. China: Chem.*, 2020, **63**, 107–115, DOI: 10.1007/s11426-019-9653-8.

174 P. Li, H. Dong, J. Xu, J. Chen, B. Jiao, X. Hou, J. Li and Z. Wu, Ligand Orientation-Induced Lattice Robustness for Highly Efficient and Stable Tin-Based Perovskite Solar Cells, *ACS Energy Lett.*, 2020, **5**, 2327–2334, DOI: 10.1021/acsenergylett.0c00960.

175 Z. Jin, B. Bin Yu, M. Liao, D. Liu, J. Xiu, Z. Zhang, E. Lifshitz, J. Tang, H. Song and Z. He, Enhanced efficiency and stability in Sn-based perovskite solar cells with secondary crystallization growth, *J. Energy Chem.*, 2021, **54**, 414–421, DOI: 10.1016/j.jechem.2020.06.044.

176 Z. Zhang, L. Wang, A. Kumar Baranwal, S. Razey Sahamir, G. Kapil, Y. Sanehira, M. Akmal Kamarudin, K. Nishimura, C. Ding, D. Liu, Y. Li, H. Li, M. Chen, Q. Shen, T. S. Ripolles, J. Bisquert and S. Hayase, Enhanced efficiency and stability in Sn-based perovskite solar cells by trimethylsilyl halide surface passivation, *J. Energy Chem.*, 2022, **71**, 604–611, DOI: 10.1016/j.jechem.2022.03.028.

177 A. Koliogiorgos, S. Baskoutas and I. Galanakis, Electronic and gap properties of Sb and Bi based halide perovskites: an ab-initio study, *Comput. Condens. Matter*, 2018, **14**, 161–166, DOI: 10.1016/j.cocom.2018.02.001.

178 I. Kopacic, B. Friesenbichler, S. F. Hoefler, B. Kunert, H. Plank, T. Rath and G. Trimmel, Enhanced Performance of Germanium Halide Perovskite Solar Cells through Compositional Engineering, *ACS Appl. Energy Mater.*, 2018, **1**, 343–347, DOI: 10.1021/acsaem.8b00007.

179 M. Chen, M. G. Ju, H. F. Garces, A. D. Carl, L. K. Ono, Z. Hawash, Y. Zhang, T. Shen, Y. Qi, R. L. Grimm, D. Pacifici, X. C. Zeng, Y. Zhou and N. P. Padture, Highly stable and efficient all-inorganic lead-free perovskite solar cells with native-oxide passivation, *Nat. Commun.*, 2019, **10**, 16, DOI: 10.1038/s41467-018-07951-y.

180 Raghvendra, R. R. Kumar and S. K. Pandey, Performance evaluation and material parameter perspective of eco-friendly highly efficient CsSnGeI3 perovskite solar cell, *Superlattices Microstruct.*, 2019, **135**, 106273, DOI: 10.1016/j.spmi.2019.106273.

181 A. Raj, M. Kumar, H. Bherwani, A. Gupta and A. Anshul, Evidence of improved power conversion efficiency in lead-free CsGeI 3 based perovskite solar cell heterostructure via scaps simulation, *J. Vac. Sci. Technol. B*, 2021, **39**, 12401, DOI: 10.1116/6.0000718.

182 S. Bhatt, R. Shukla, C. Pathak and S. K. Pandey, Evaluation of performance constraints and structural optimization of a core-shell ZnO nanorod based eco-friendly perovskite solar cell, *Sol. Energy*, 2021, **215**, 473–481, DOI: 10.1016/j.solener.2020.12.069.

183 N. Singh, A. Agarwal and M. Agarwal, Numerical simulation of highly efficient lead-free perovskite layers for the application of all-perovskite multi-junction solar cell, *Superlattices Microstruct.*, 2021, **149**, 106750, DOI: 10.1016/j.spmi.2020.106750.

184 X. Meng, T. Tang, R. Zhang, K. Liu, W. Li, L. Yang, Y. Song, X. Ma, Z. Cheng and J. Wu, Optimization of germanium-based perovskite solar cells by SCAPS simulation, *Opt. Mater.*, 2022, **128**, 112427, DOI: 10.1016/j.optmat.2022.112427.

185 D. Saikia, J. Bera, A. Betal and S. Sahu, Performance evaluation of an all inorganic CsGeI3 based perovskite

solar cell by numerical simulation, *Opt. Mater.*, 2022, **123**, 111839, DOI: 10.1016/j.optmat.2021.111839.

186 A. Jain, O. Voznyy and E. H. Sargent, High-Throughput Screening of Lead-Free Perovskite-like Materials for Optoelectronic Applications, *J. Phys. Chem. C*, 2017, **121**, 7183–7187, DOI: 10.1021/acs.jpcc.7b02221.

187 P. Karuppuswamy, K. M. Boopathi, A. Mohapatra, H. C. Chen, K. T. Wong, P. C. Wang and C. W. Chu, Role of a hydrophobic scaffold in controlling the crystallization of methylammonium antimony iodide for efficient lead-free perovskite solar cells, *Nano Energy*, 2018, **45**, 330–336, DOI: 10.1016/j.nanoen.2017.12.051.

188 F. Jiang, D. Yang, Y. Jiang, T. Liu, X. Zhao, Y. Ming, B. Luo, F. Qin, J. Fan, H. Han, L. Zhang and Y. Zhou, Chlorine-Incorporation-Induced Formation of the Layered Phase for Antimony-Based Lead-Free Perovskite Solar Cells, *J. Am. Chem. Soc.*, 2018, **140**, 1019–1027, DOI: 10.1021/jacs.7b10739.

189 A. Singh, K. M. Boopathi, A. Mohapatra, Y. F. Chen, G. Li and C. W. Chu, Photovoltaic Performance of Vapor-Assisted Solution-Processed Layer Polymorph of Cs3Sb2I9, *ACS Appl. Mater. Interfaces*, 2018, **10**, 2566–2573, DOI: 10.1021/acsami.7b16349.

190 A. Singh, R. Chaurasiya, A. Bheemaraju, J. S. Chen and S. Satapathi, Strain-Induced Band-Edge Modulation in Lead-Free Antimony-Based Double Perovskite for Visible-Light Absorption, *ACS Appl. Energy Mater.*, 2021, **4**, 3926–3932, DOI: 10.1021/acsaem.1c03598.

191 Y. Liu, Q. Chen, A. Mei, B. Hu, Z. Yang and W. Chen, Bandgap aligned Cu 12 Sb 4 S 13 quantum dots as efficient inorganic hole transport materials in planar perovskite solar cells with enhanced stability, *Sustainable Energy Fuels*, 2019, **3**, 831–840, DOI: 10.1039/c9se00003h.

192 F. S. Freitas, A. S. Gonçalves, A. De Morais, J. E. Benedetti and A. F. Nogueira, Graphene-like MoS2 as a low-cost counter electrode material for dye-sensitized solar cells, *NanoGe J. Energy Sustain.*, 2012, 11002–11003, DOI: 10.1039/c0xx00000x.

193 J. Li, Y. Lv, H. Han, J. Xu and J. Yao, Two-Dimensional Cs3Sb2I9−xClx Film with (201) Preferred Orientation for Efficient Perovskite Solar Cells, *Materials*, 2022, **15**, 2883, DOI: 10.3390/ma15082883.

194 K. Ahmad, M. Q. Khan and H. Kim, Simulation and fabrication of all-inorganic antimony halide perovskite-like material based Pb-free perovskite solar cells, *Opt. Mater.*, 2022, **128**, 112374, DOI: 10.1016/J.OPTMAT.2022.112374.

195 F. Bai, Y. Hu, Y. Hu, T. Qiu, X. Miao and S. Zhang, Lead-free, air-stable ultrathin Cs3Bi2I9 perovskite nanosheets for solar cells, *Sol. Energy Mater. Sol. Cells*, 2018, **184**, 15–21, DOI: 10.1016/j.solmat.2018.04.032.

196 D. B. Khadka, Y. Shirai, M. Yanagida and K. Miyano, Tailoring the film morphology and interface band offset of caesium bismuth iodide-based Pb-free perovskite solar cells, *J. Mater. Chem. C*, 2019, **7**, 8335–8343, DOI: 10.1039/c9tc02181g.

197 M. S. Shadabroo, H. Abdizadeh and M. R. Golobostanfard, Elpasolite structures based on A2AgBiX6 (A: MA, Cs, X: I, Br): application in double perovskite solar cells, *Mater. Sci. Semicond. Process.*, 2021, **125**, 105639, DOI: 10.1016/j.mssp.2020.105639.

198 W. Hu, X. He, Z. Fang, W. Lian, Y. Shang, X. Li, W. Zhou, M. Zhang, T. Chen, Y. Lu, L. Zhang, L. Ding and S. Yang, Bulk heterojunction gifts bismuth-based lead-free perovskite solar cells with record efficiency, *Nano Energy*, 2020, **68**, 104362, DOI: 10.1016/j.nanoen.2019.104362.